ANASTASIA CASSISA

Study of neutron rich Si isotopes with ACTAR TPC detector

LISE campaign 2022

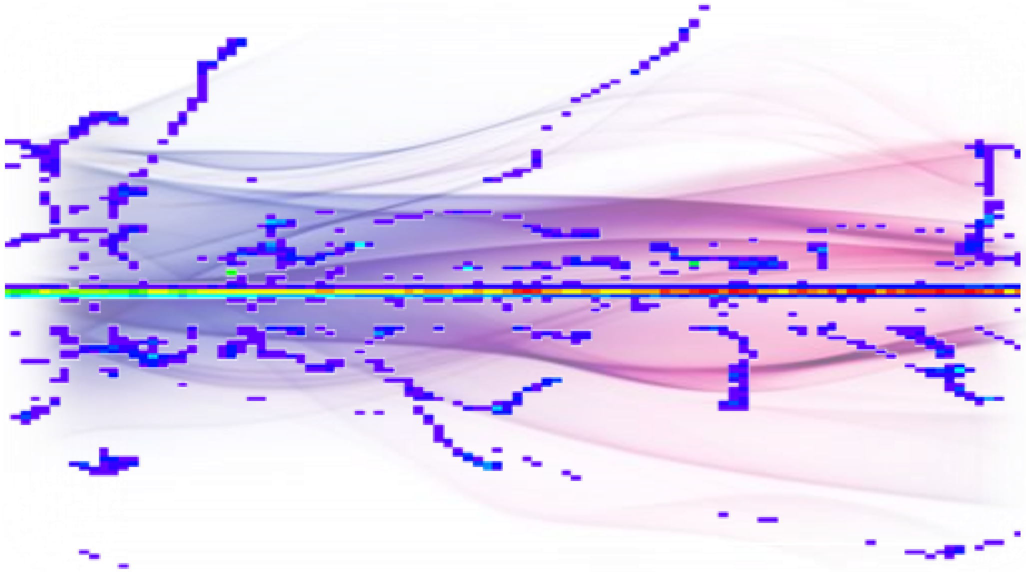

Nuclear Physics Institute

CHARLES UNIVERSITY
Faculty of mathematics and physics

BARRANDE FELLOWSHIPS

GANIL
GRAND ACCELERATEUR NATIONAL D'IONS LOURDS
LABORATOIRE COMMUN DSM/CEA-IN2P3/CNRS

MŠMT
MINISTERSTVO ŠKOLSTVÍ, MLÁDEŽE A TĚLOVÝCHOVY

OUTLINES

- *Introduction* ;
- *Physical motivations* ;
- *Experimental setups* ;
- *Status of the data analysis* .

Introduction

Shell evolution far from the stability

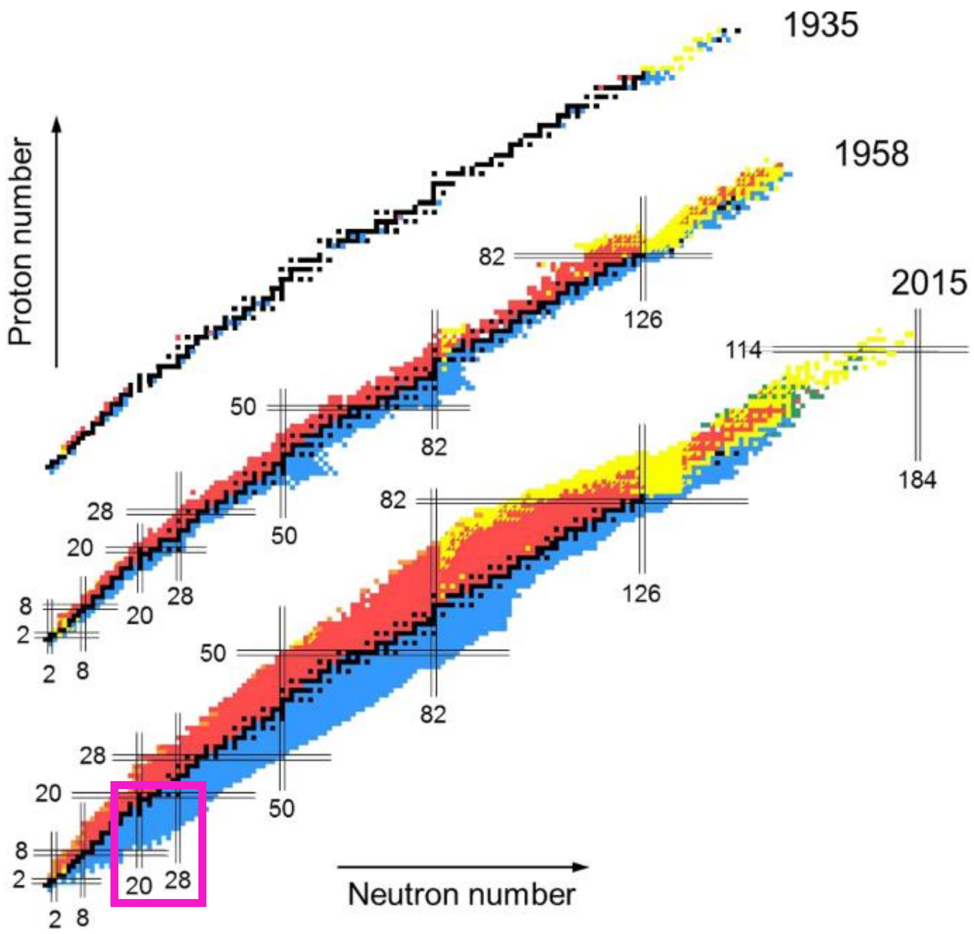

- The nuclear structure properties are governed by *the interaction between nucleons*, protons and neutrons.
- Until the 1980s, only nuclear systems close to the stability line were experimentally accessible, therefore theoretical models lacked important information on large isospin (T) values.
- Fusion-evaporation studies on systems farther from stability have challenged the classical theoretical approaches: **magic numbers are not immutable**! [*]
- Since the 1990s, with the development of *radioactive beam facilities*, detailed studies of exotic nuclei helped to reveal the effects of large isospin values in light systems.
- By experimentally determining the properties of *exotic nuclei* comprehensive theoretical models can be put to essential tests.

PHYSICAL REVIEW C VOLUME 12, NUMBER 2 AUGUST 1975

Direct measurement of the masses of ^{11}Li and $^{26-32}$Na with an on-line mass spectrometer [*]

C. Thibault, R. Klapisch, C. Rigaud, A. M. Poskanzer,* R. Prieels,† L. Lessard,‡ and W. Reisdorf§

Laboratoire René Bernas du Centre de Spectrométrie Nucléaire et de Spectrométrie de Masse, 91406 Orsay, France

(Received 17 March 1975)

The use of an on-line mass spectrometer to make direct mass measurements of short-lived isotopes far from the stability line has been improved to yield more accurate mass measurements for $^{27-30}$Na, new mass measurements for ^{11}Li, ^{31,32}Na, and to remove a discrepancy between existing mass measurements of ^{26}Na. The mass excesses (keV) measured are: ^{11}Li, 40940 ± 80; ^{26}Na, −6901 ± 25; ^{27}Na, −5620 ± 60; ^{28}Na, −1140 ± 80; ^{29}Na, 2650 ± 100; ^{30}Na, 8370 ± 200; ^{31}Na, 10600 ± 800; ^{32}Na, 16400 ± 1100. The ^{11}Li value indicates that it is bound by only 170 ± 80 keV. The masses of ^{31}Na and ^{32}Na imply that these nuclei are more tightly bound than expected from theoretical predictions.

[NUCLEAR STRUCTURE ^{11}Li, $^{26-32}$Na; measured atomic masses. On-line mass spectrometer.
RADIOACTIVITY ^{11}Li; deduced logft.]

How to extend the chart of nuclides?
G. G. Adamian, N. V. Antonenko, A. Diaz-Torres, S. Heinz; Eur. Phys. J. A (2020) 56:47

Grand Accélérateur National d’Ions Lourds (GANIL)

LISE spectrometer at GANIL

Grand Accélérateur National d'Ions Lourds (GANIL)

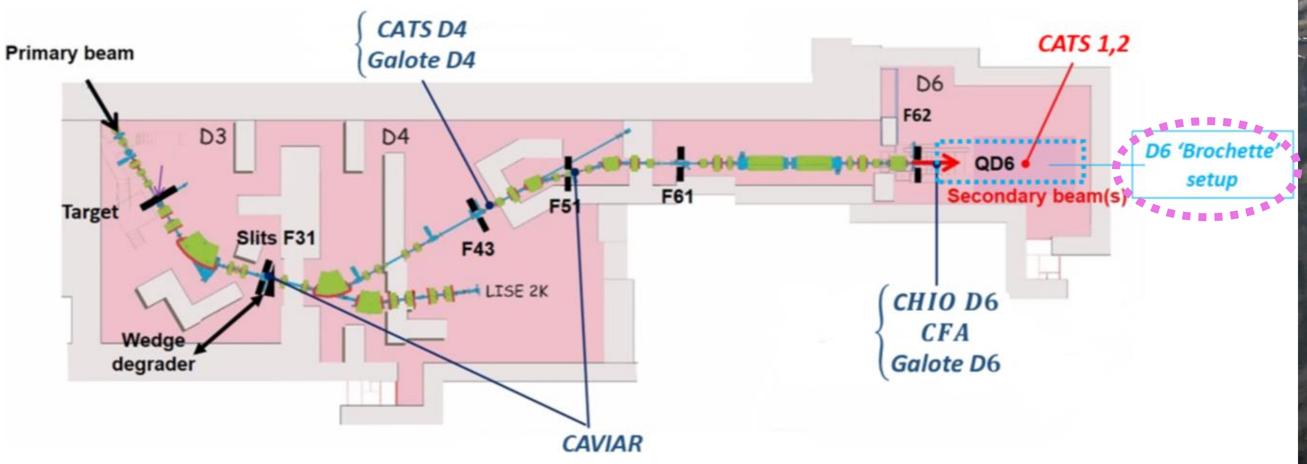

Physical motivations

Shell closure indications

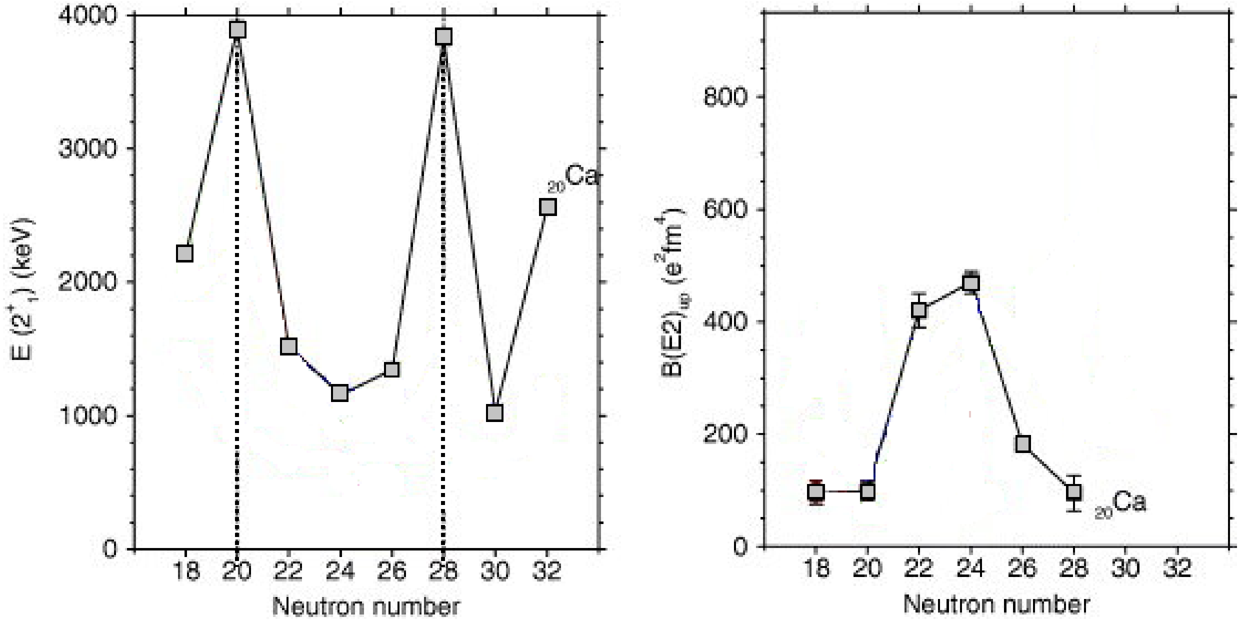

Evolution of the *N* = 28 shell closure: a test bench for nuclear forces, O Sorlin and M-G Porquet, 2012

Shell closure indications

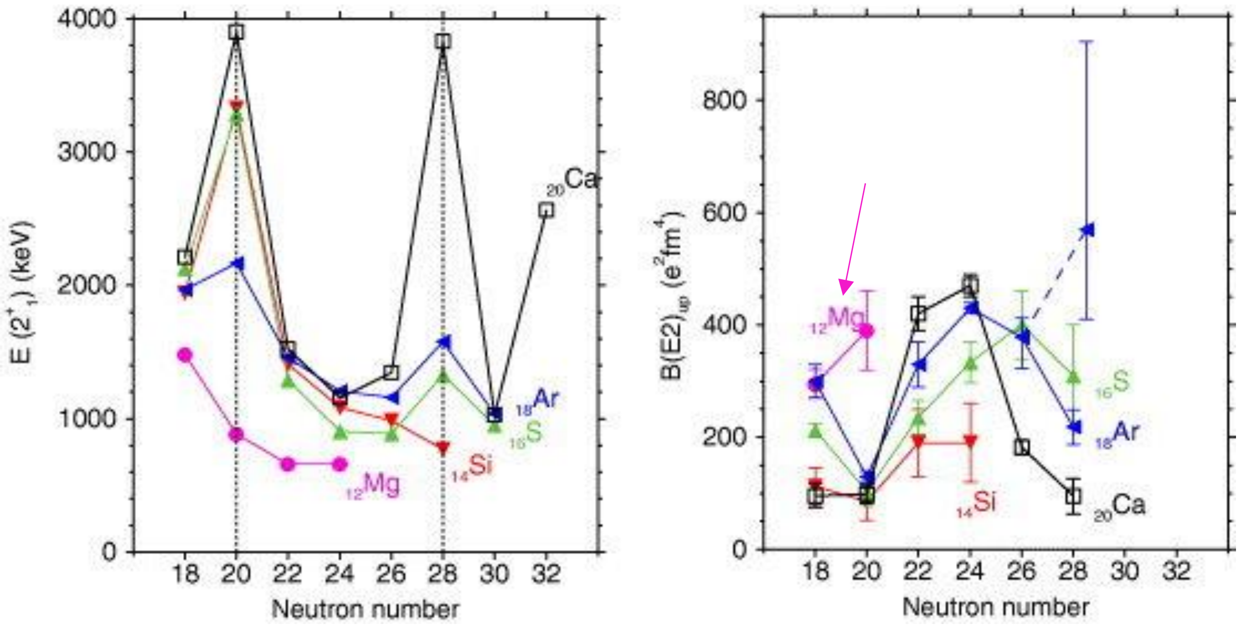

Evolution of the N = 28 shell closure: a test bench for nuclear forces, O Sorlin and M-G Porquet, 2012

Island of inversion and loss of magicity

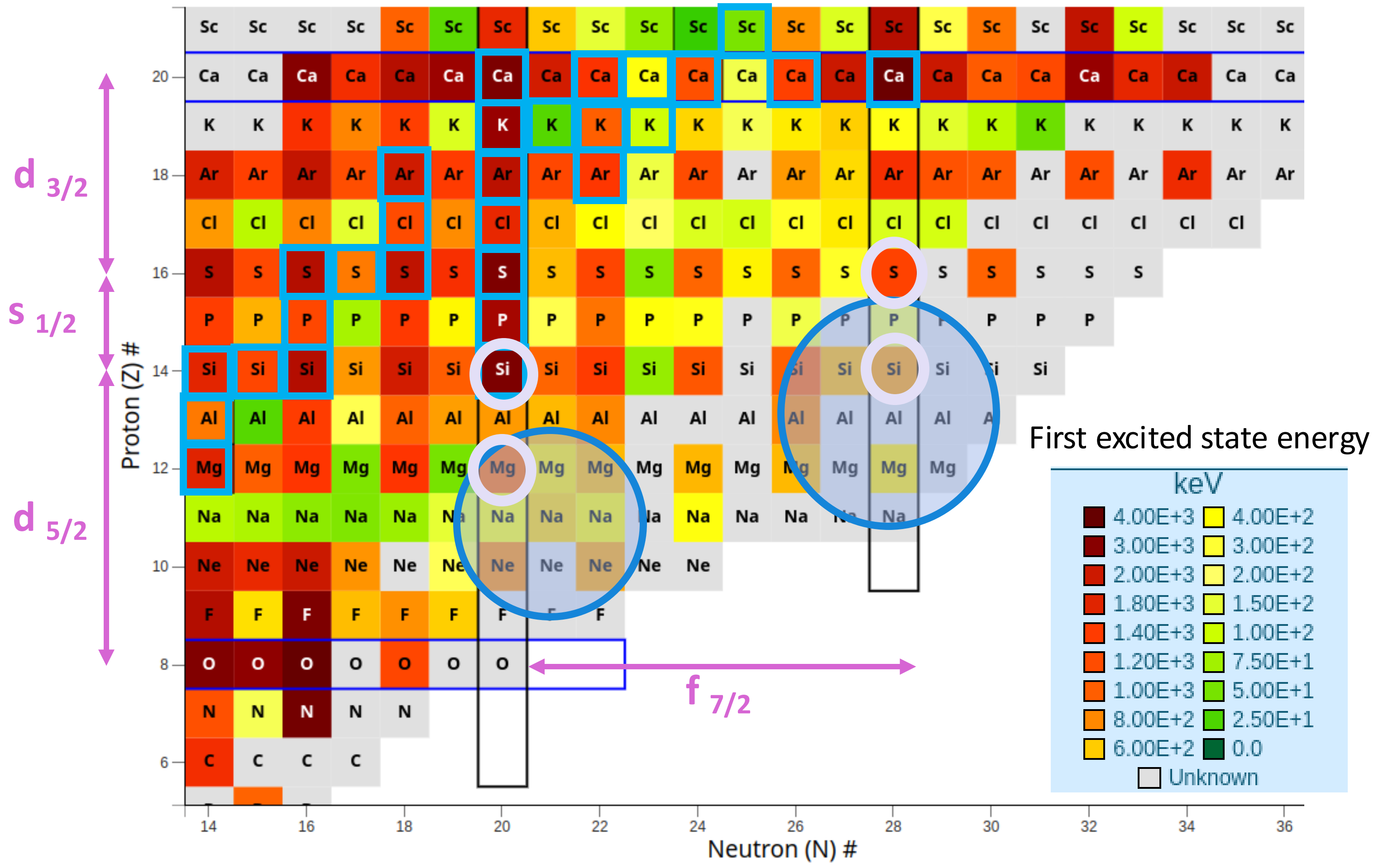

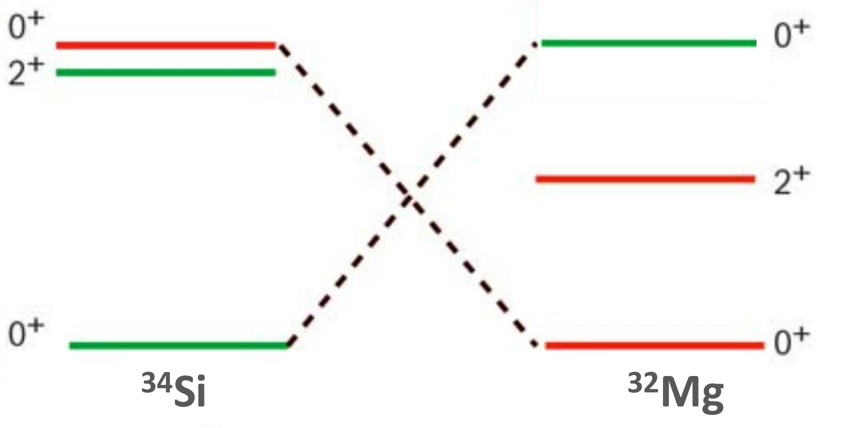

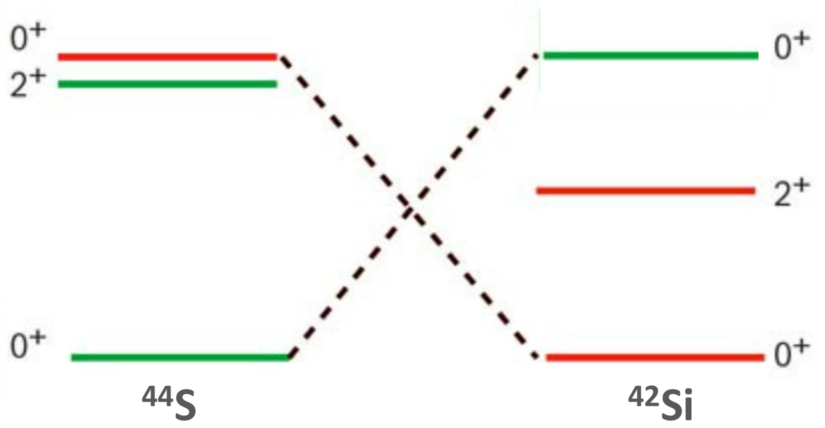

Islands of insight in the nuclear chart; B. Alex Brown; 2013

Island of inversion and loss of magicity

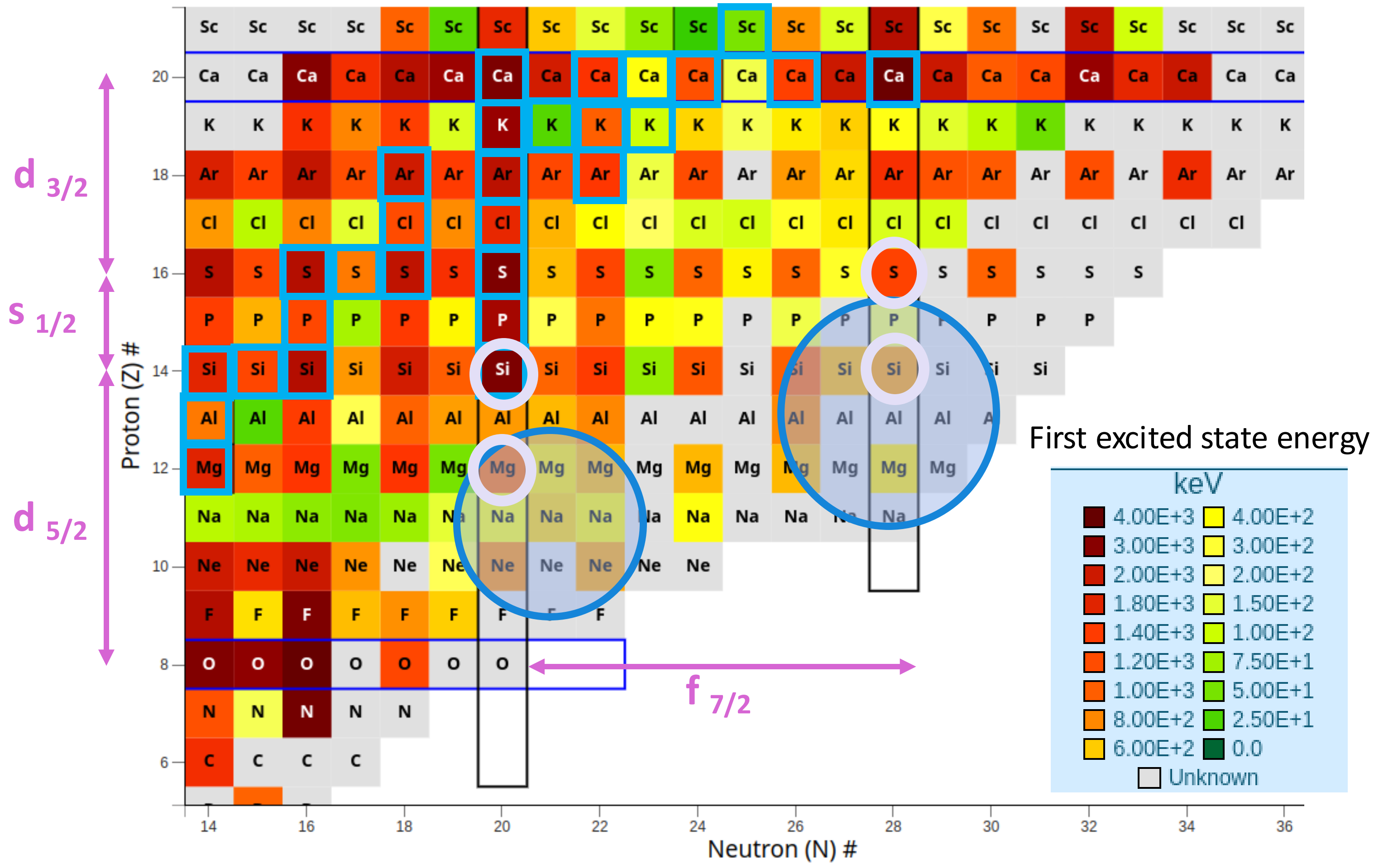

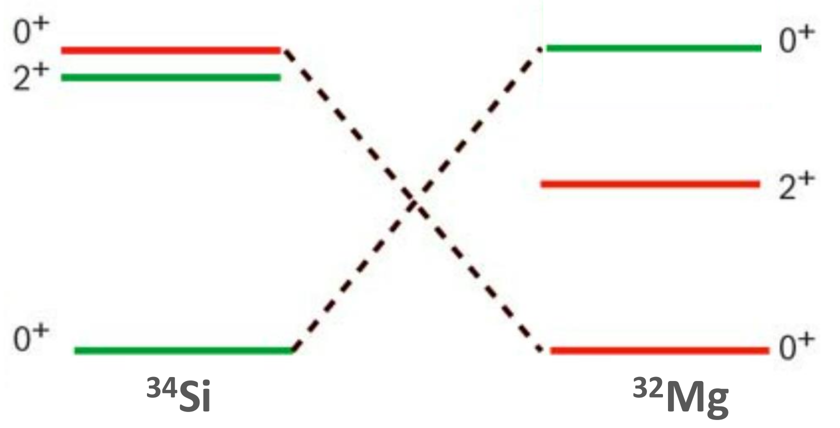

- Gradual **reduction of N=20 shell gap** as one approaches the neutron drip line;
- The configuration for the protons suddenly changing from “closed shell like” in ^{34}Si to “open shell like” in ^{32}Mg, which leads to stronger **proton-neutron correlations**.

Islands of insight in the nuclear chart; B. Alex Brown; 2013

Shape transition and shell evolution

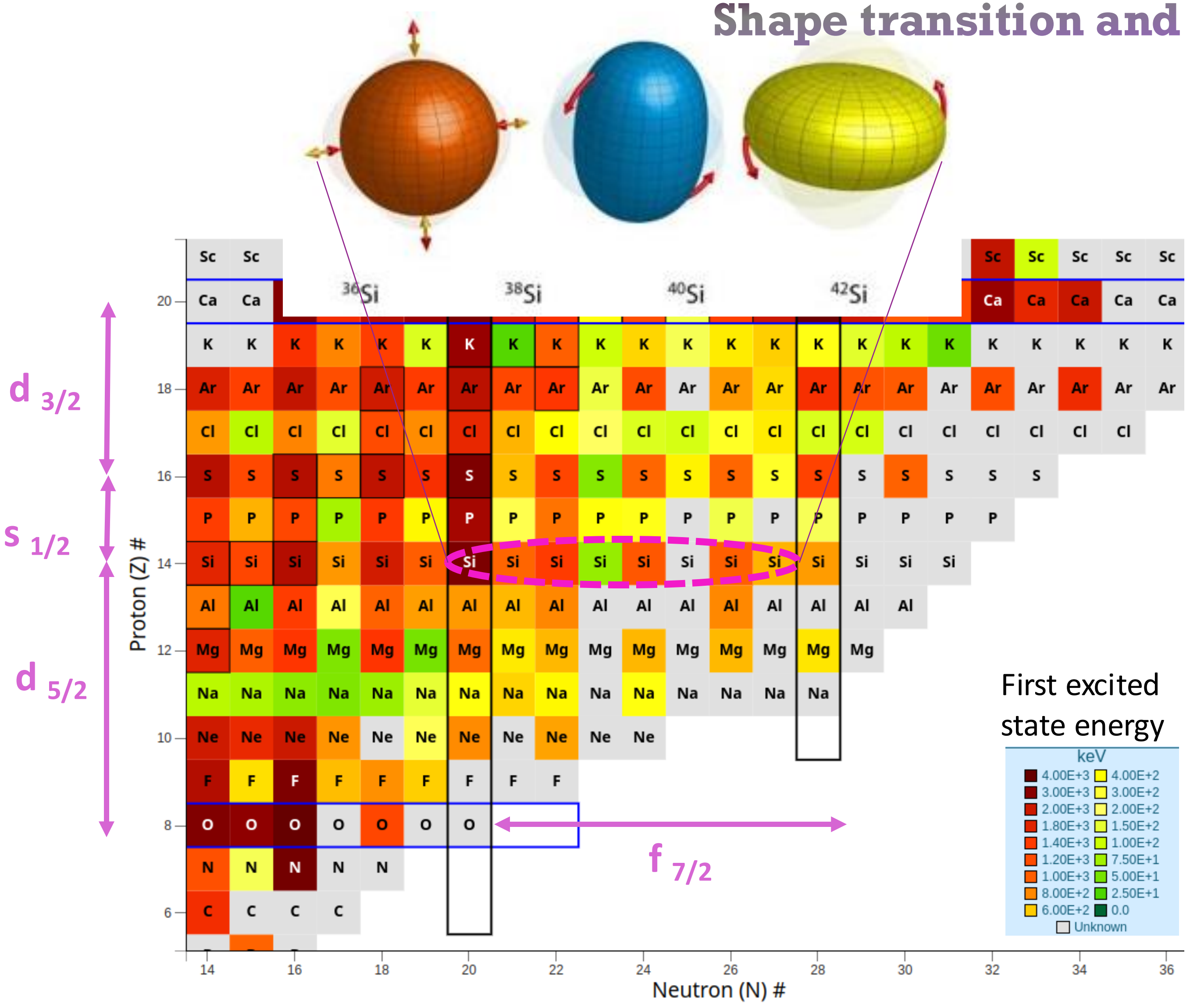

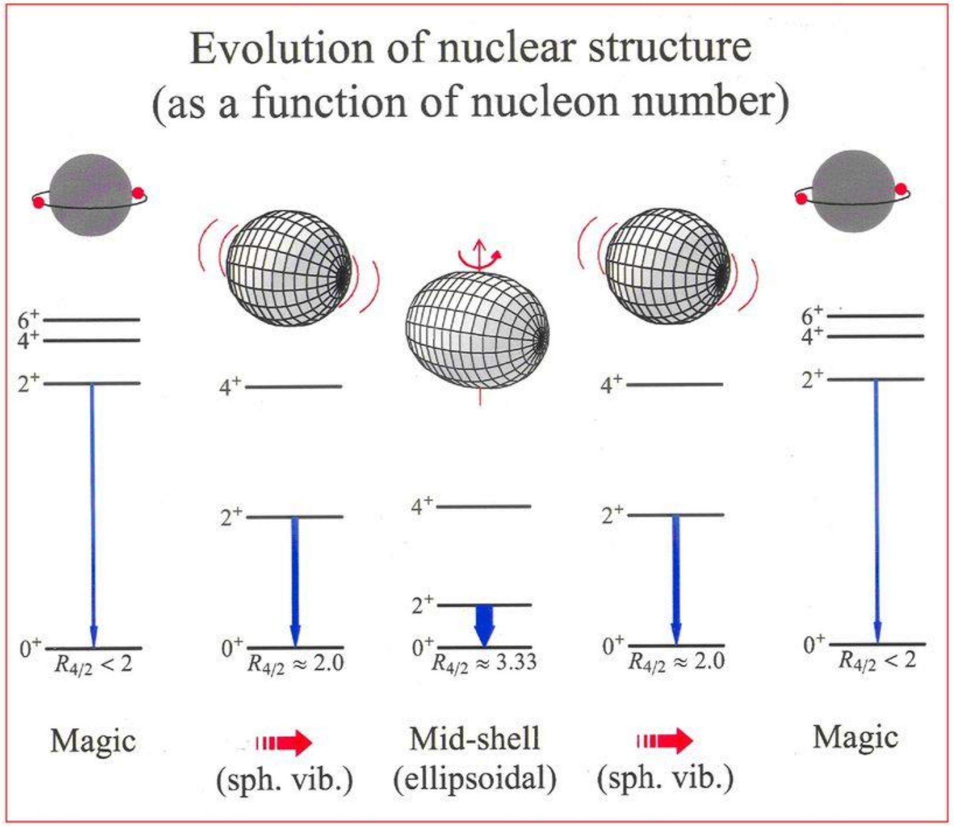

Evolution of the N=28 shell closure: a test bench for nuclear forces, O. Sorlin, M.-G. Porquet 2012

Shape transition and shell evolution

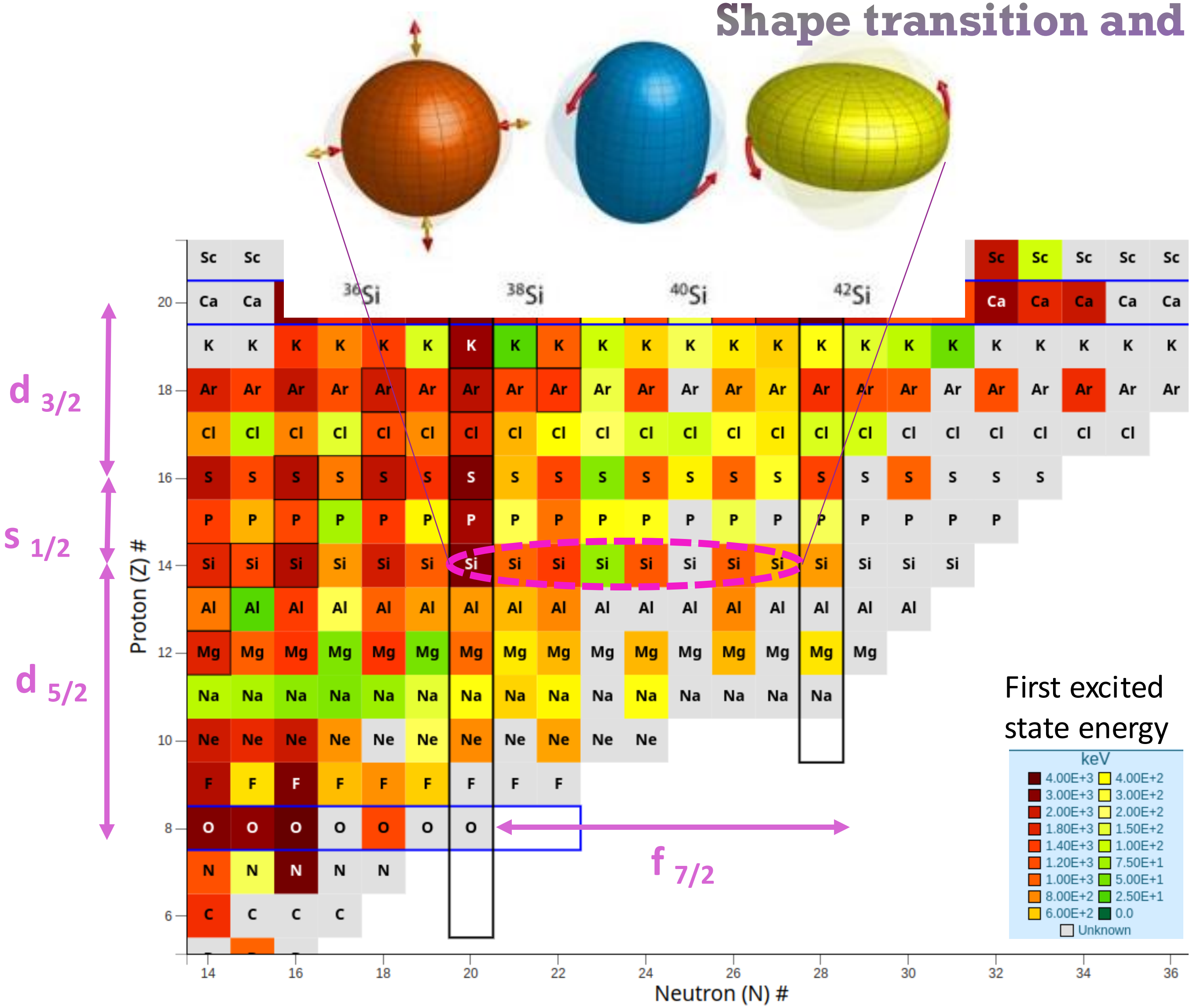

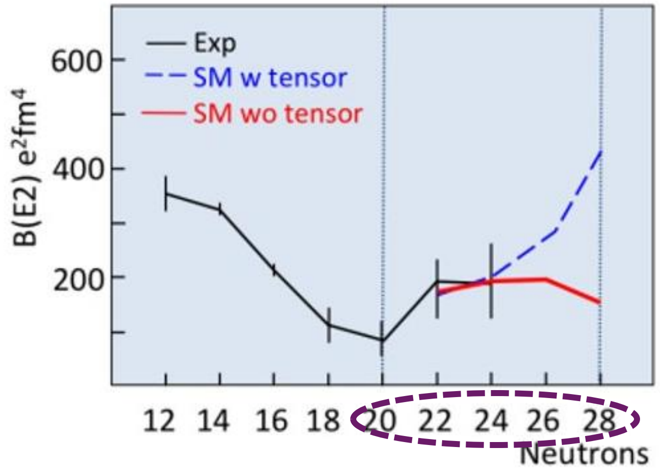

$$\beta_2 = \frac{4\pi}{3zR_0^2}\left[\frac{B(E2)}{e^2}\right]^{1/2}$$

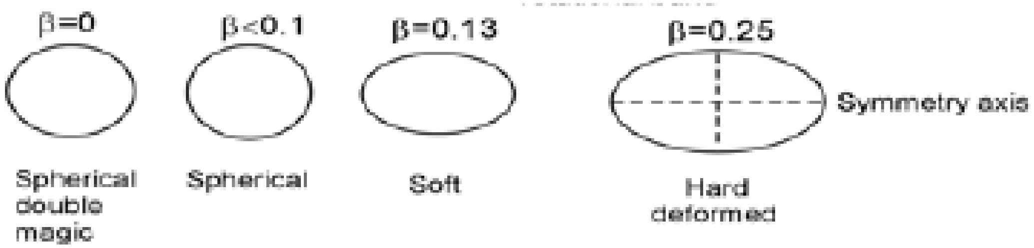

Evolution of the N=28 shell closure: a test bench for nuclear forces, O. Sorlin, M.-G. Porquet 2012

Derivation of the Mn/Mp ratio in exotic nuclei

Nuclear excitations

- Multipole 2^+ transition matrix element

$$M = b_n^F M_n + b_p^F M_p$$

The parameters $b_{n(p)}$ represent the external-field neutron (proton) interaction strengths.

$$M = \langle J_f, T_f, T_{fz} || O_L^F || J_i, T_i, T_{iz} \rangle$$

$$M_{n(p)} = \int \rho_{fi}^{n(p)}(r) r^{l-2} dr$$

$$\frac{M_n}{M_p} \sim \frac{N}{Z} \frac{\beta_n}{\beta_p}$$

- A priori for homogeneous collective model Mn/Mp = N/Z
- $\mathbf{M_p}$ can be checked by direct comparison of the microscopic calculations to charge transition densities measured by electron scattering (e,e'), or with COULEX experiments.
- $\mathbf{M_n}$ can be determined by (p,p') scattering.

The ratios of the neutron and proton transition matrix elements (Mn/Mp) were studied for 0^+ -> 2^+ transitions in single-closed-shell (SCS) nuclei by comparing inelastic hadron scattering and electromagnetic transition rates.

Field	Energy	bn/bp
EM	-	0
p	10-50MeV	~3
n	10-50MeV	~1/3

For EM transition b_n=0 and b_p=1

Bernstein, A. M. et al. (1983) Comments Nucl. Part. Phys., 11, 203215

Bernstein, A. M. et al. (1981) Physics Letters B, 103, 255258

From the cross section to the Mn/Mp ratio

From the elastic (p,p) analysis:

- Entrance channel potential;

From the inelastic (p,p') analysis:

- Neutron transition matrix, Mn;

From the COULEX EXCITATION analysis:

- Proton transition matrix, Mp;

$$B(E2, J_i \to J_f) = e^2 \frac{1}{(2J_i + 1)} |M_p|$$

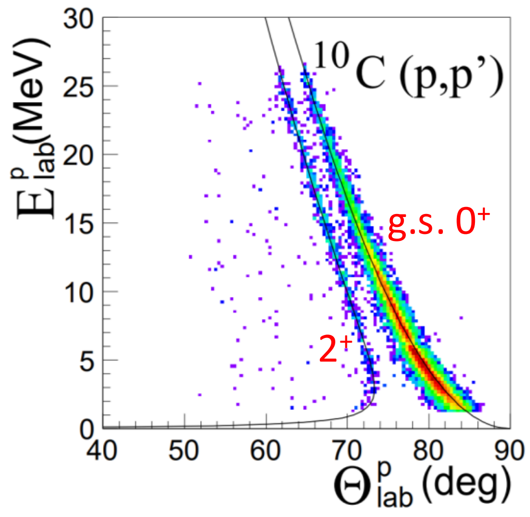

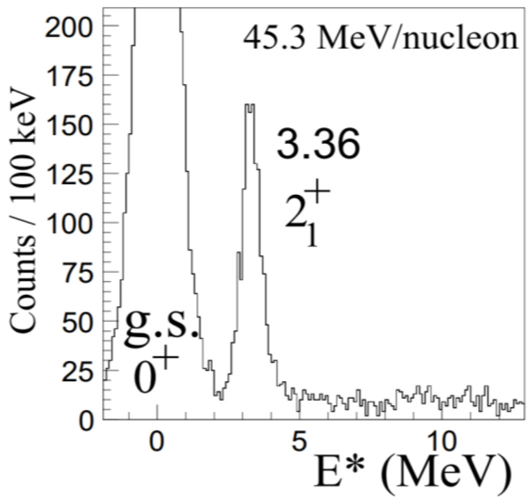

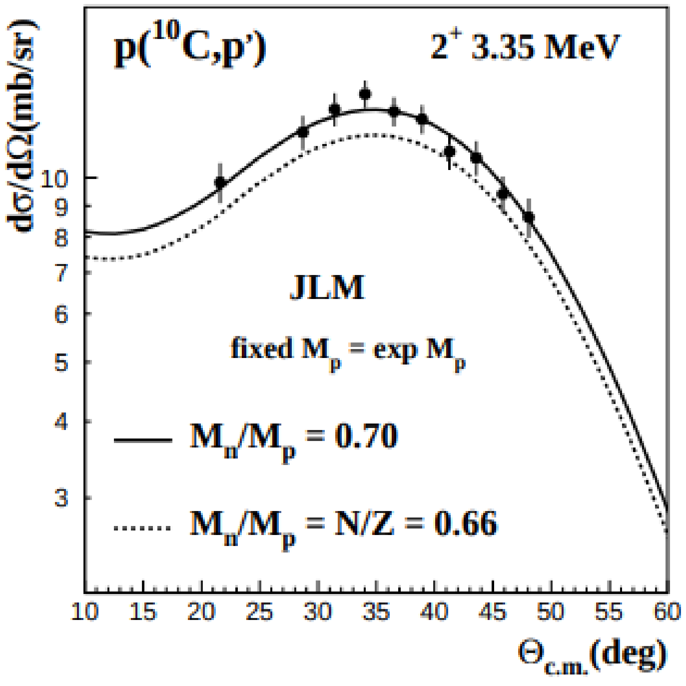

$$\frac{M_n}{M_p} = \frac{b_p}{b_n}\left[\frac{(\beta_p R)_{pp'}}{(\beta_n R)_{em}}\left(1 + \frac{b_n N}{b_p Z}\right) - 1\right]$$

Generalized Bernstein Formula

N Alamanos et al 1998 J.. Inelastic proton scattering and nuclear structure towards the drip lines. Phys. G: Nucl. Part. Phys. 24 1541

C. Jouanne, V. Lapoux, F. Auger, N. Alamanos, A. Drouart, et al.. Structure of low-lying states of 10,11C from proton elastic and inelastic scattering. Physical Review C, 2005, 72, pp.014308.ff10.1103/PhysRevC.72.014308ff. ffin2p3-00024409f

Experimental setups

"Brochette" setup

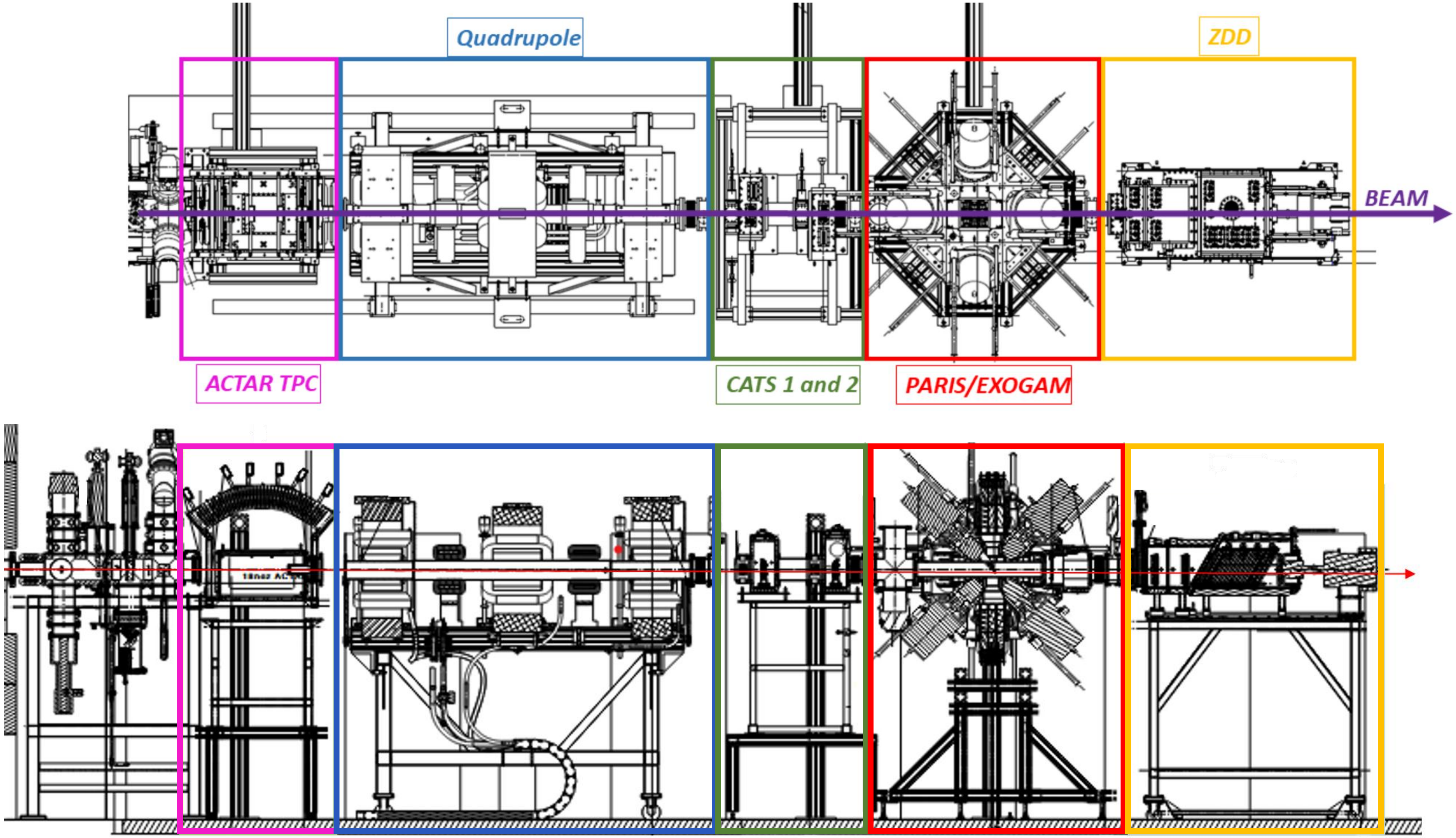

ACtive TARget Time Projection Chamber setup

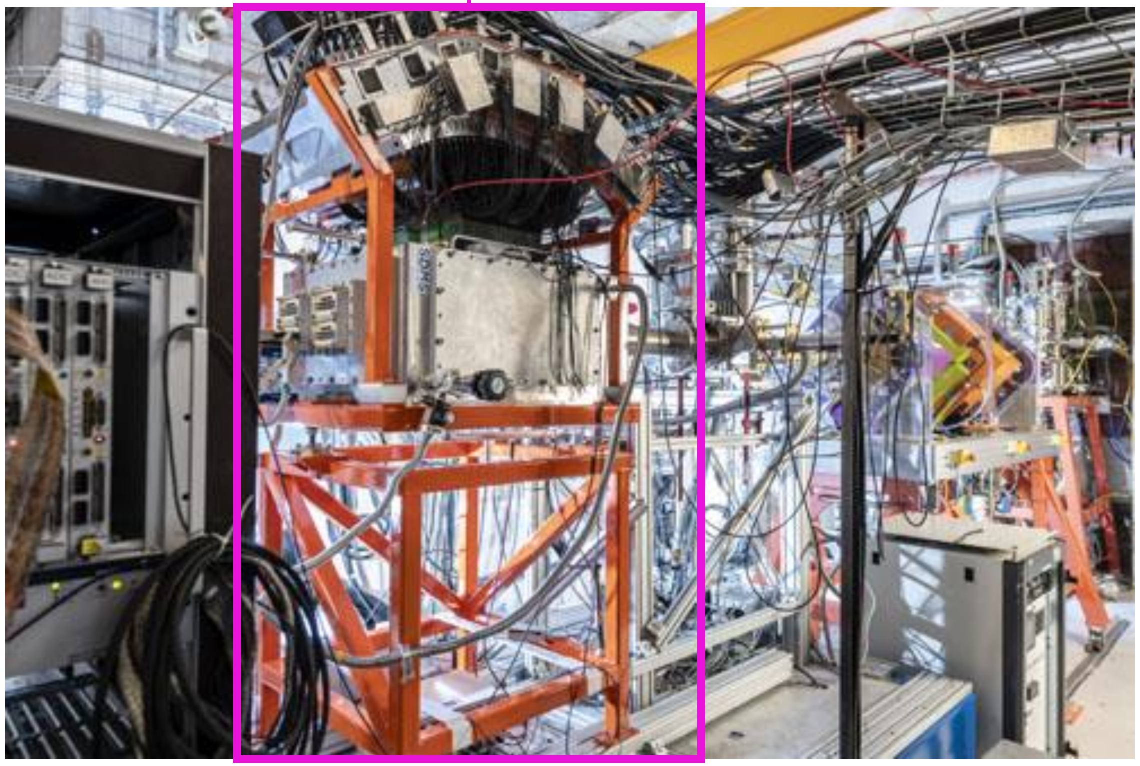

The ACTAR TPC chamber and me during the setup mounting process.

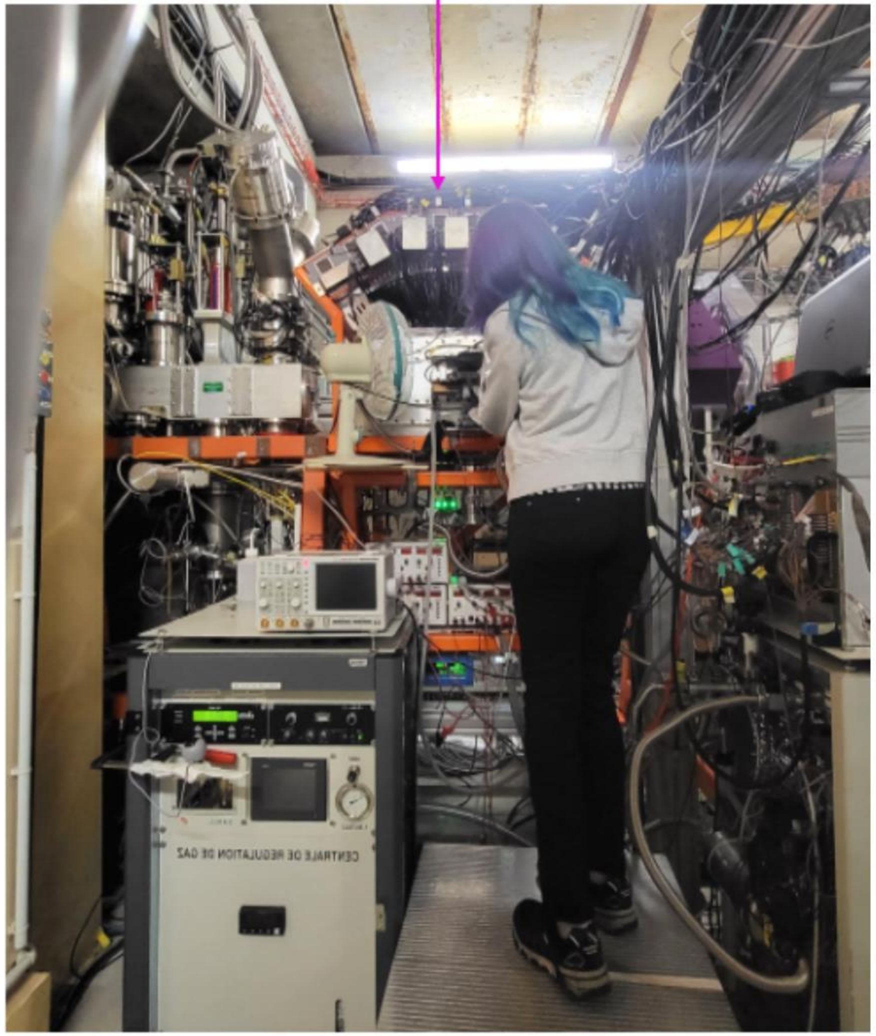

PAD plane ACTAR TPC

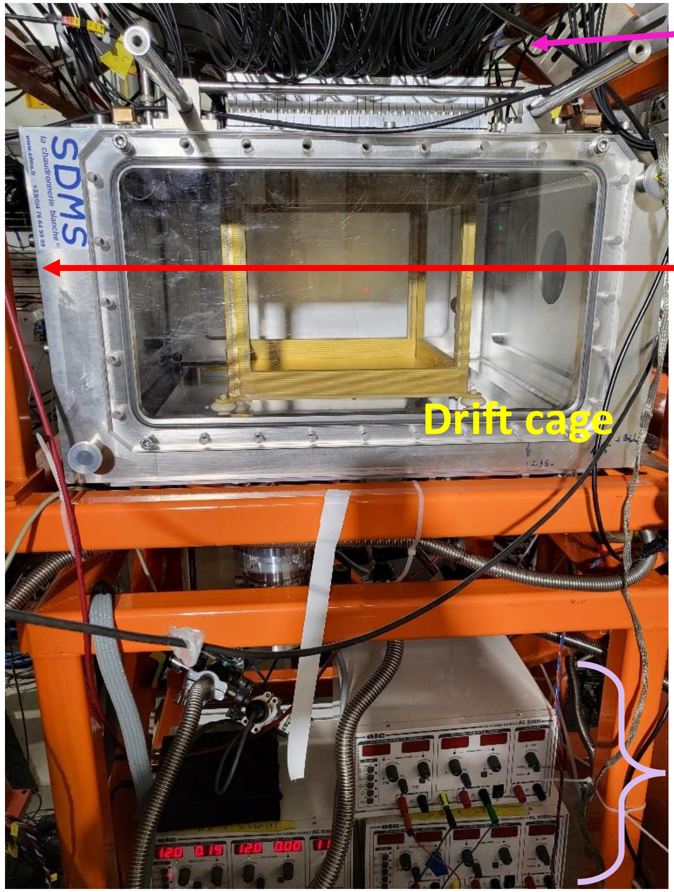

Beam

20 µm diameter
1 mm spacing

Low voltage for Silicon detectors and for the PAD plane

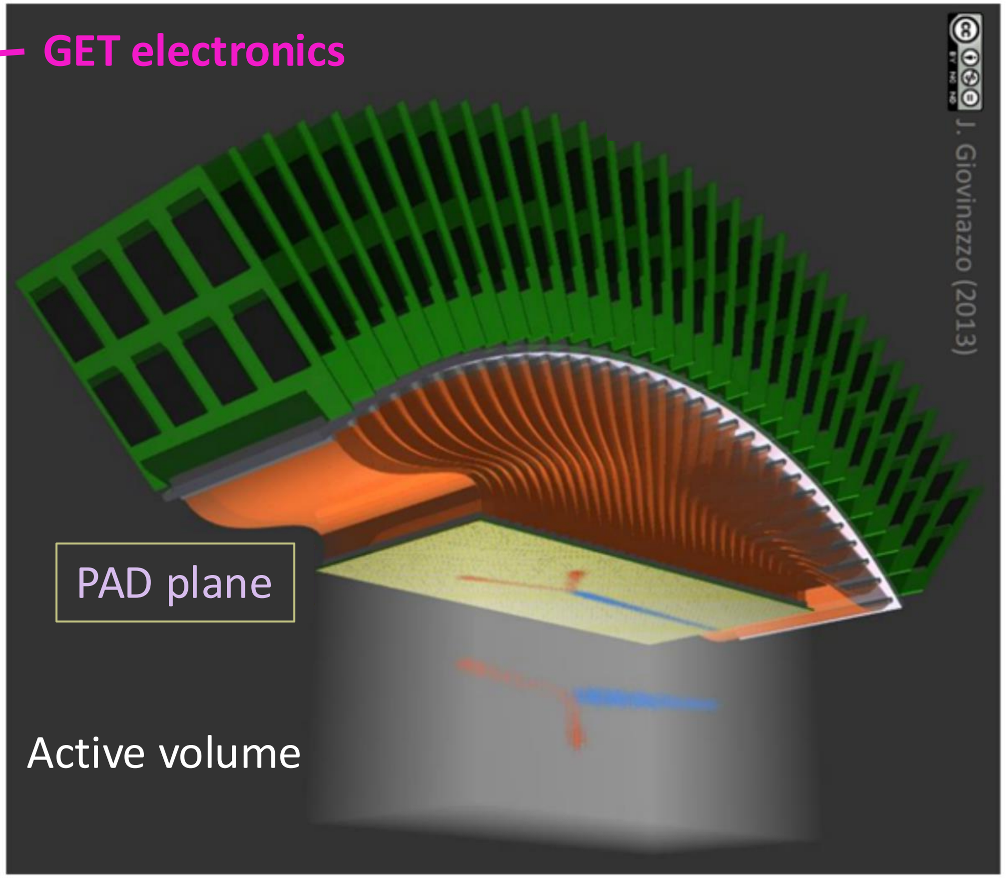

ACTAR TPC performance with GET electronics; J. Giovinazzo, J. Pancin, J. Pibernat, T. Roger; 2020

PAD plane ACTAR TPC

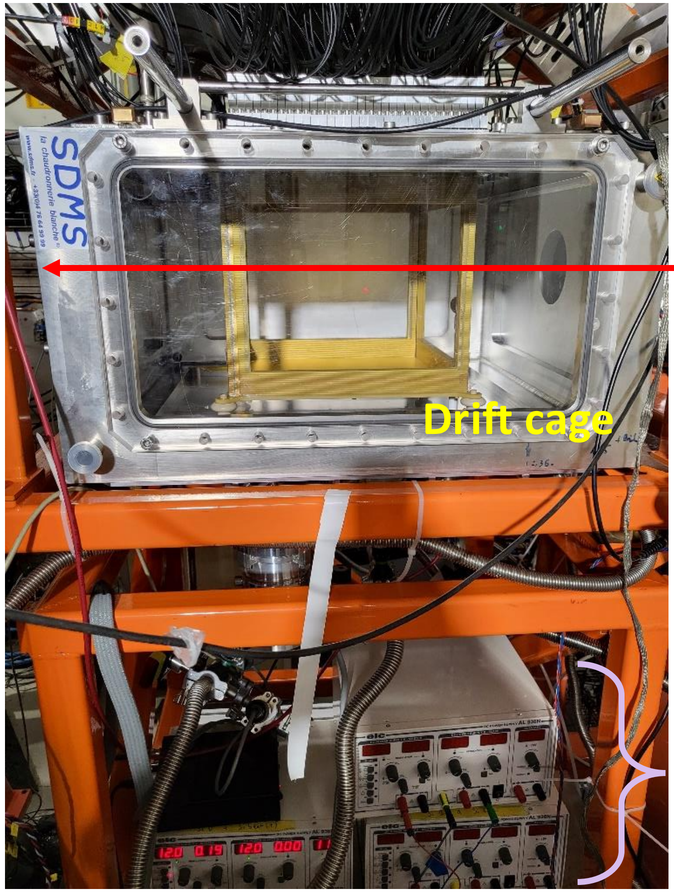

20 µm diameter
1 mm spacing

Low voltage for Silicon detectors and for the PAD plane

The charge projection plane is segmented in 128x128 square pads of 2x2 mm2 connected directly to the GET (General Electronics for TPCs project) system.

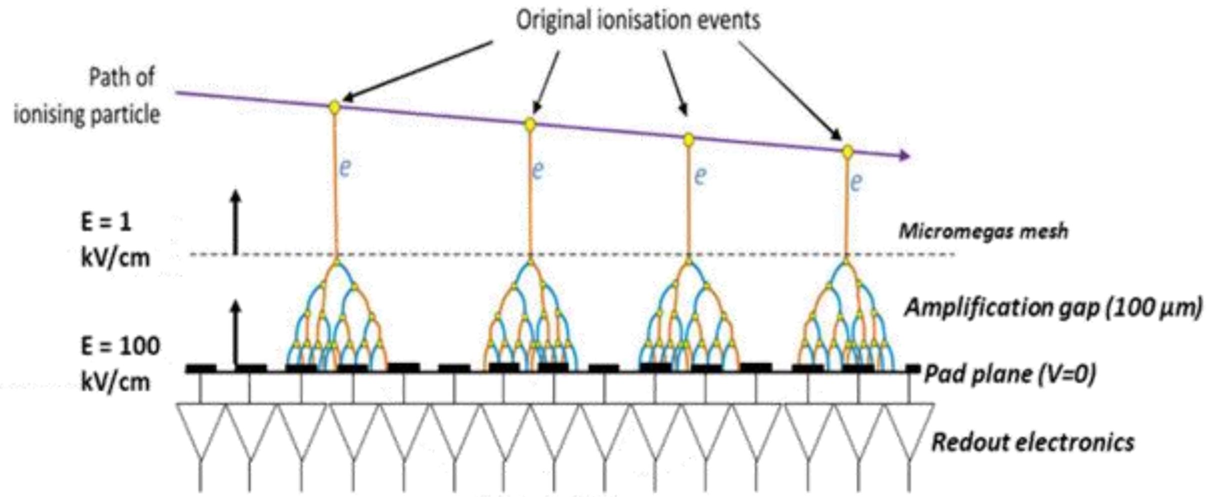

ACTAR TPC performance with GET electronics; J. Giovinazzo, J. Pancin, J. Pibernat, T. Roger; 2020

Si detectors setup

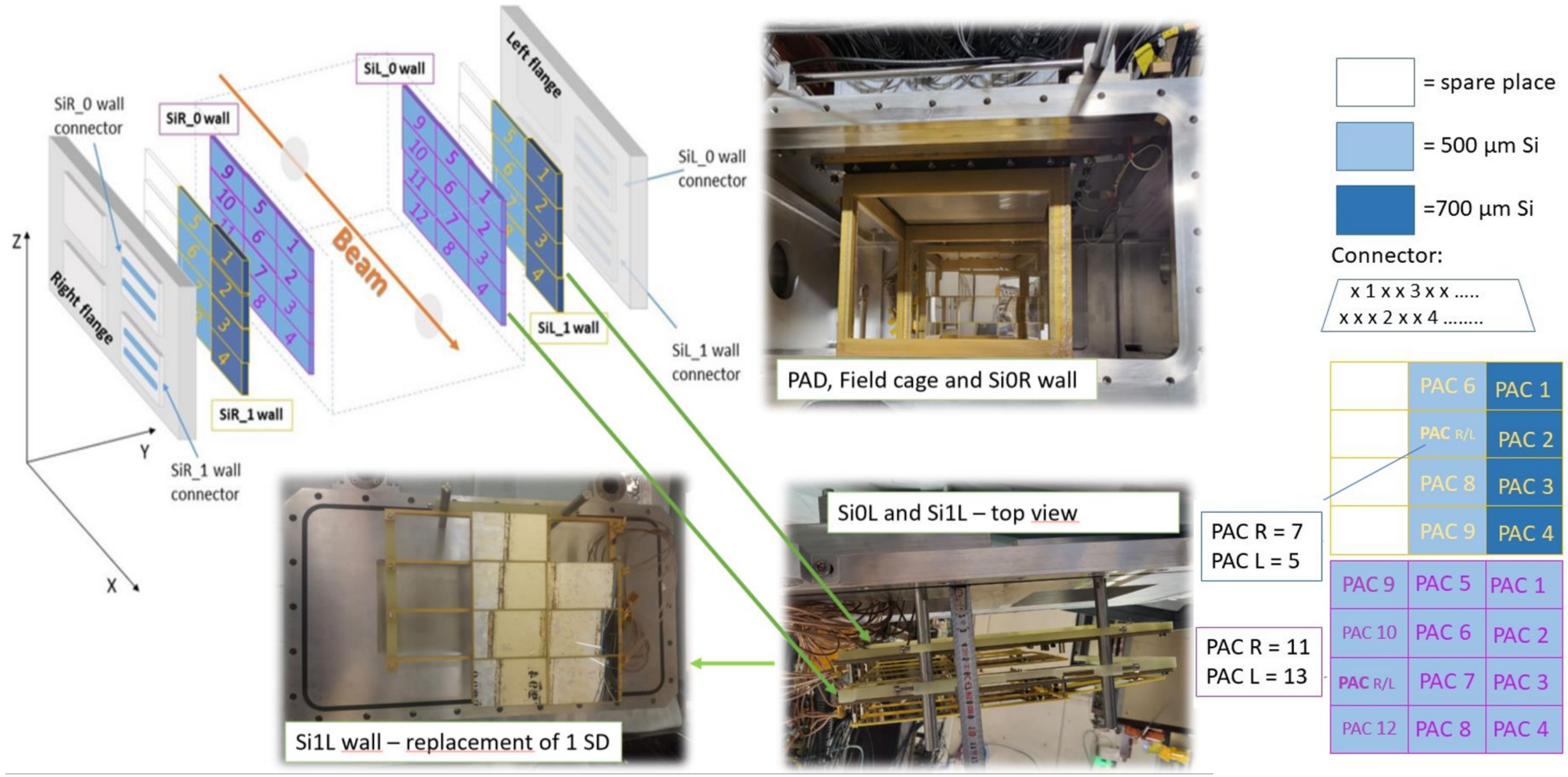

$^{34,36,38}Si(p,p')^{34,36,38}Si^{*}$ (Ex 2^{+})

ACTAR TPC gas mixture:

Isobutane (C_4H_{10}) 10%

H_2 90%

Pressure = 980 mbar

Si HV = 50 V

ACTAR settings:

V_{mesh} = -610 V

V_{drift} = -6000 V

V_{low} = -610 V

V_{pads} = -90 V

TRIGGER = Si0R + Si0L & CFA

Event by event information

PAD plane ACTAR TPC

Si detectors

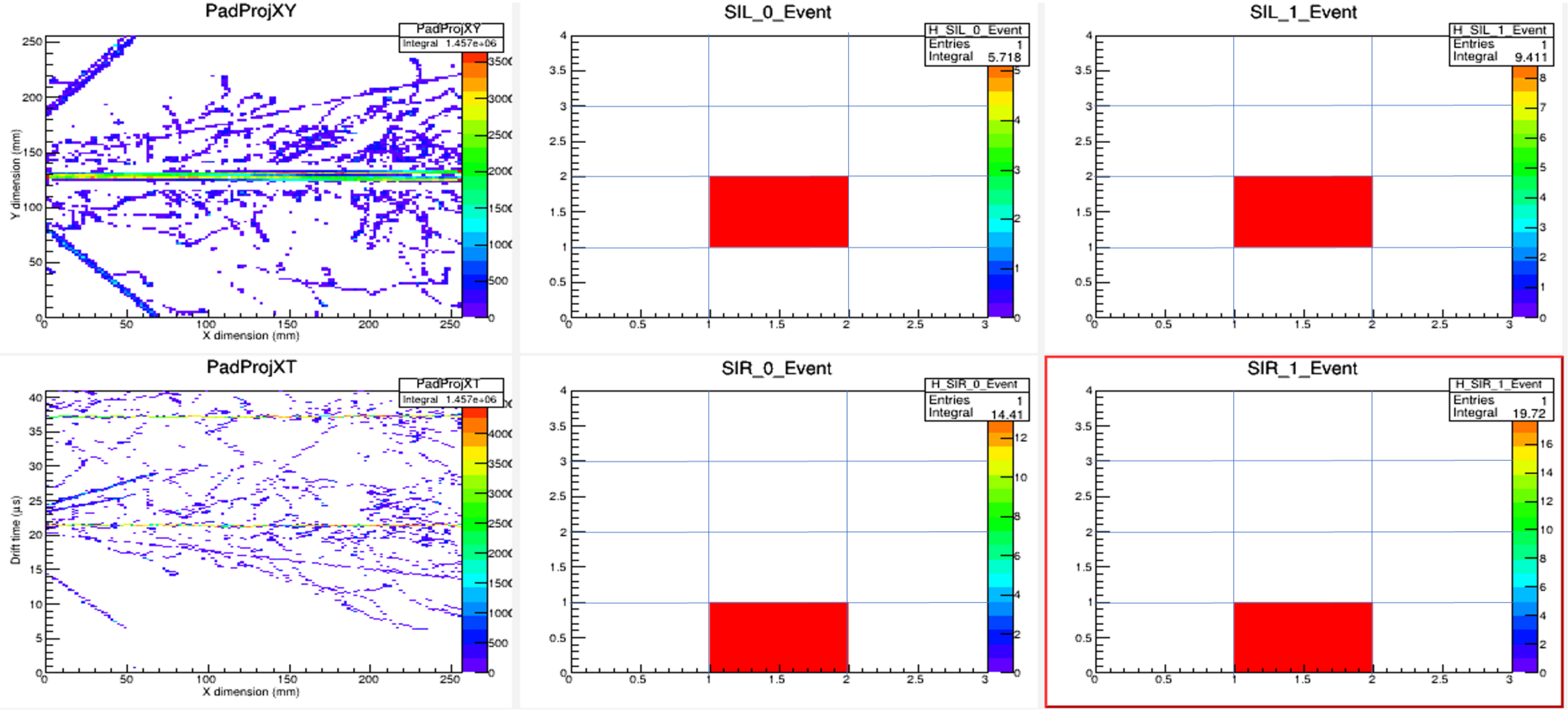

Data analysis

Data analysis structure

Beam production and identification → Lise beam consisting of different ions requires a proper identification.

↓

Proton detection → The reaction products can be identified using the pad plane of ACTAR and the silicon detectors.

↓

Kinematics and excitation energy spectra → To obtain the kinematics information it' necessary the tracks reconstruction.

↓

Cross sections → The (p,p) and (p,p') cross section analysis give us the proper parameters to extract the Mn/Mp ratio.

Beam production and identification

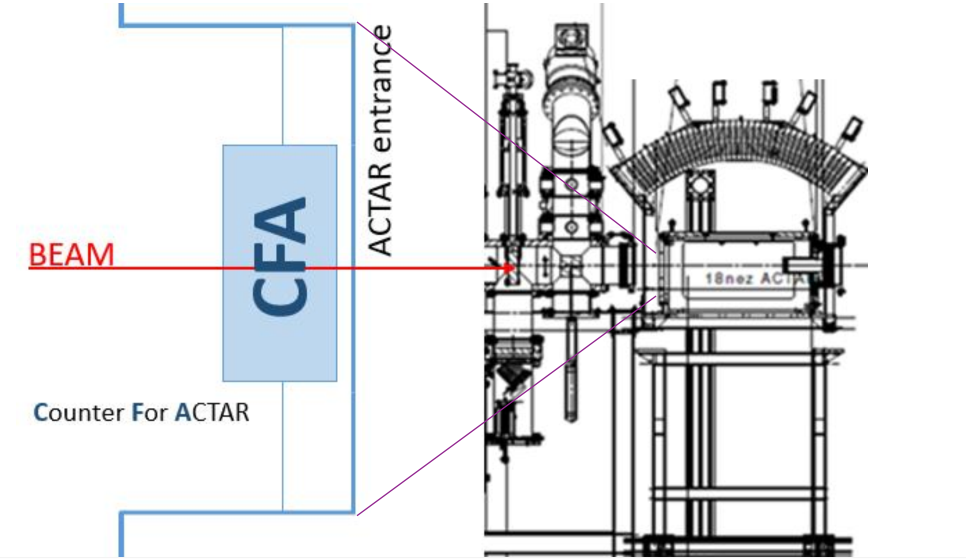

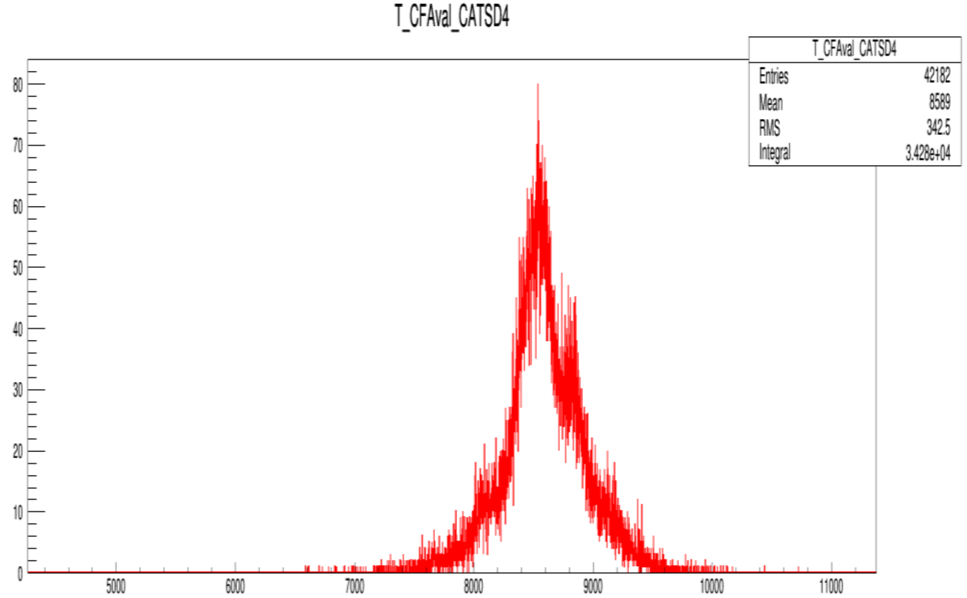

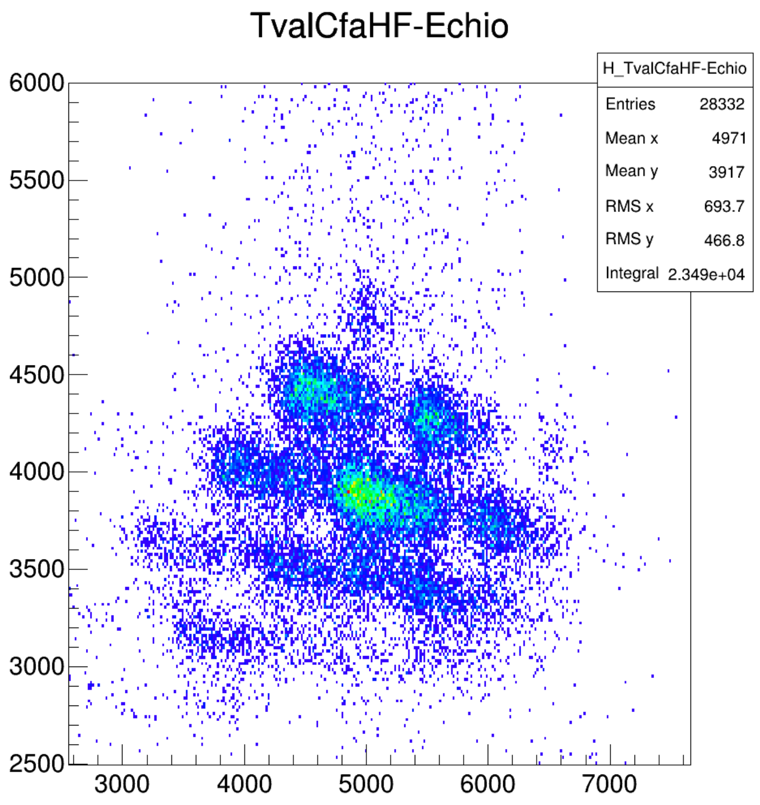

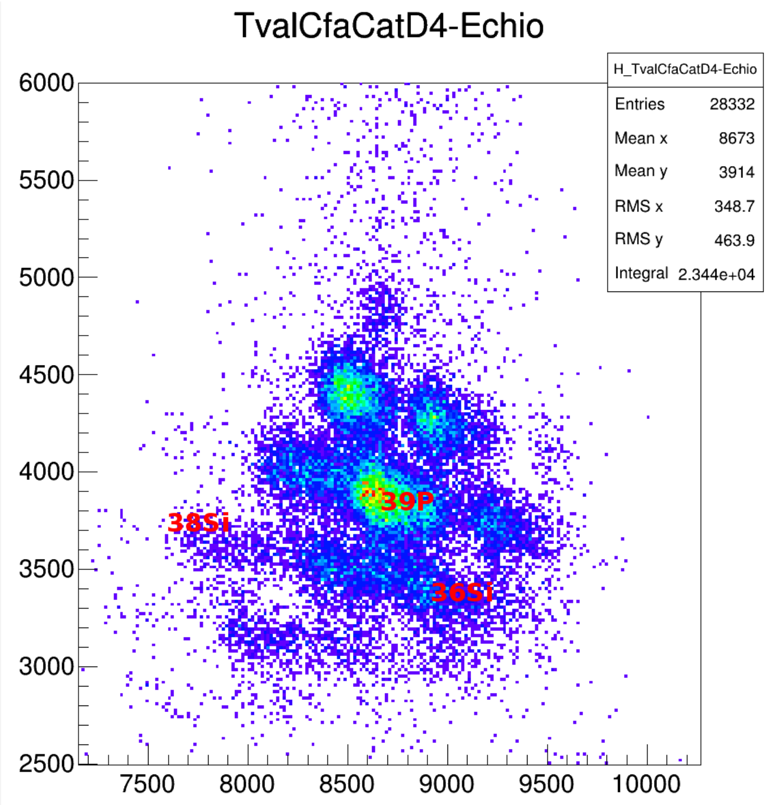

We used a 60 MeV/u ^{48}Ca primary beam with an intensity of 4μA on about 700 μm Be target to produce $^{34,36,38}Si$, using the LISE spectrometer.

Particle Identification: ΔE-E silicon telescope detectors

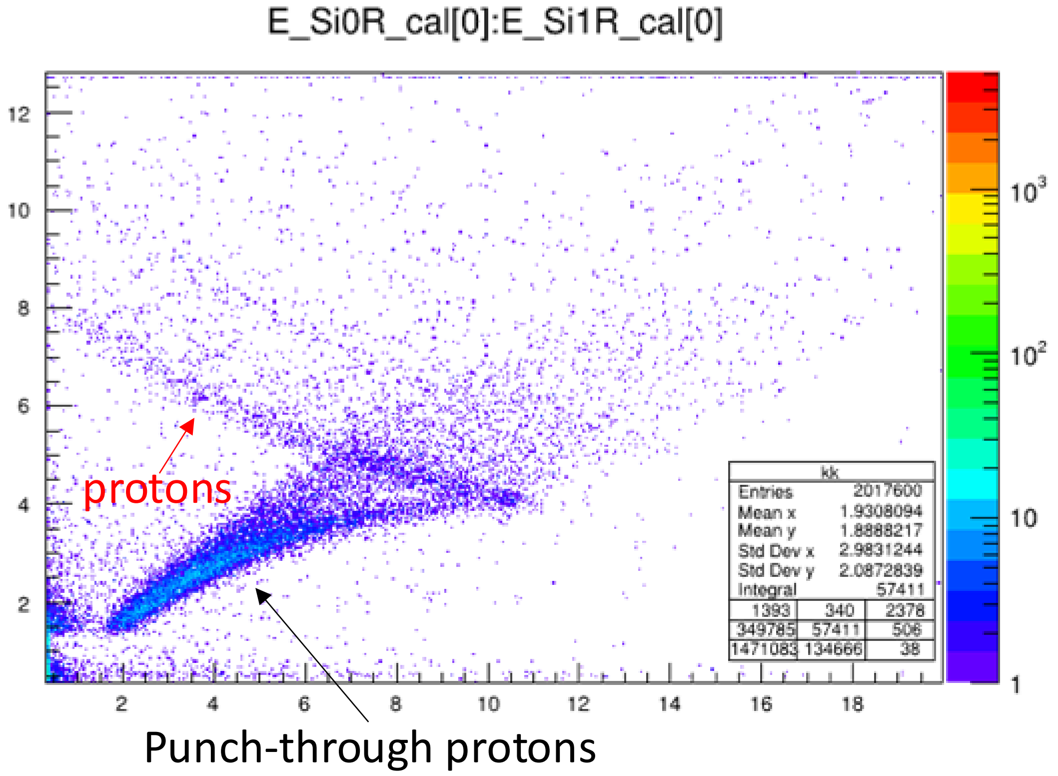

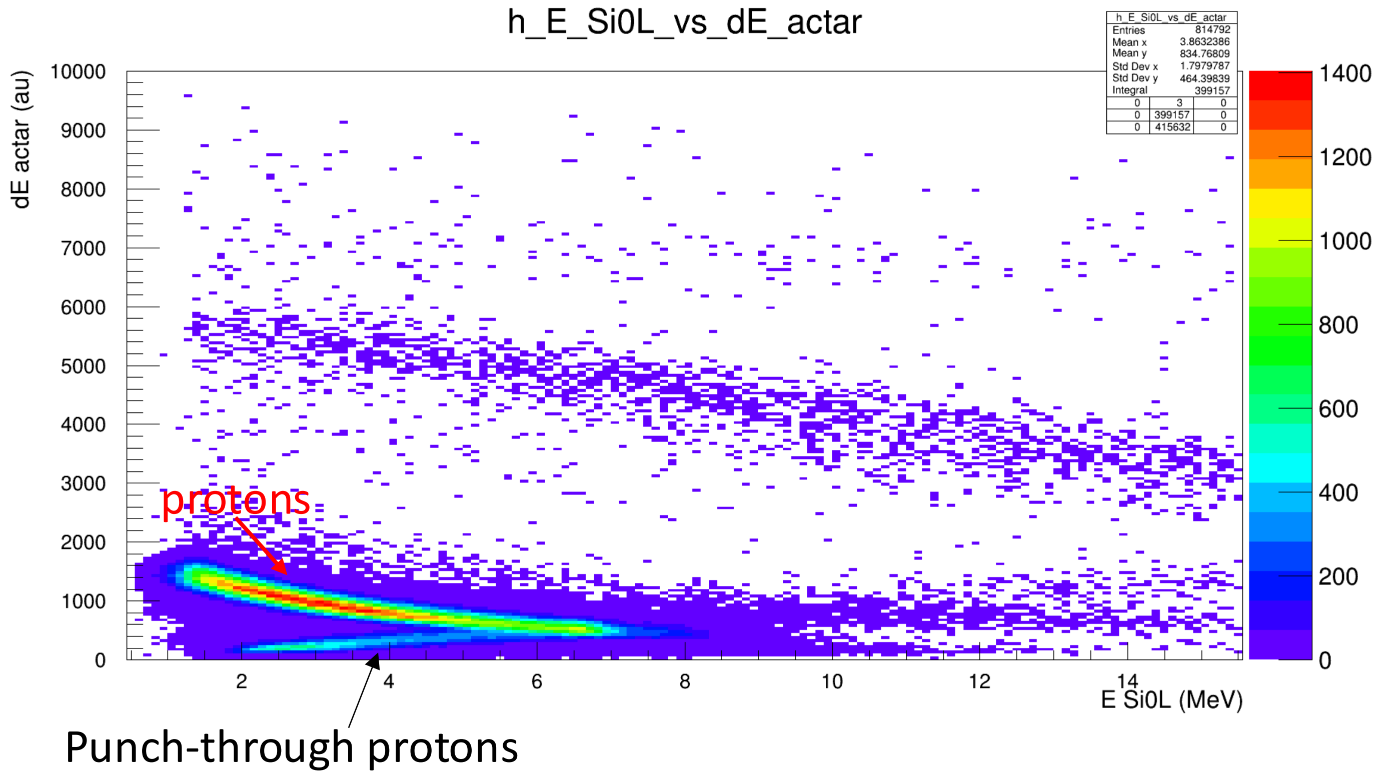

Cluster Algorithm

Cluster Algorithm steps:

- Tracks reconstruction: it scans the space and fill a matrix with the pads volume (VOXELS) containing charge;
- Kinematics conditions: the data points are saved as clusters.
- Fit of the clusters.

Kinematics conditions:

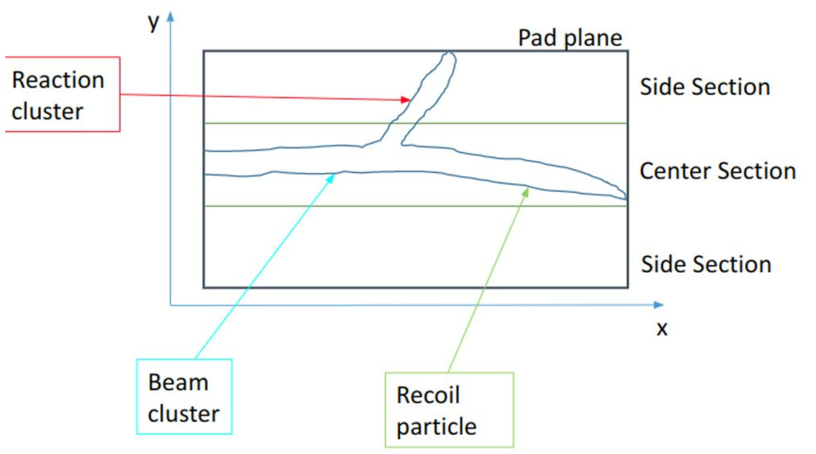

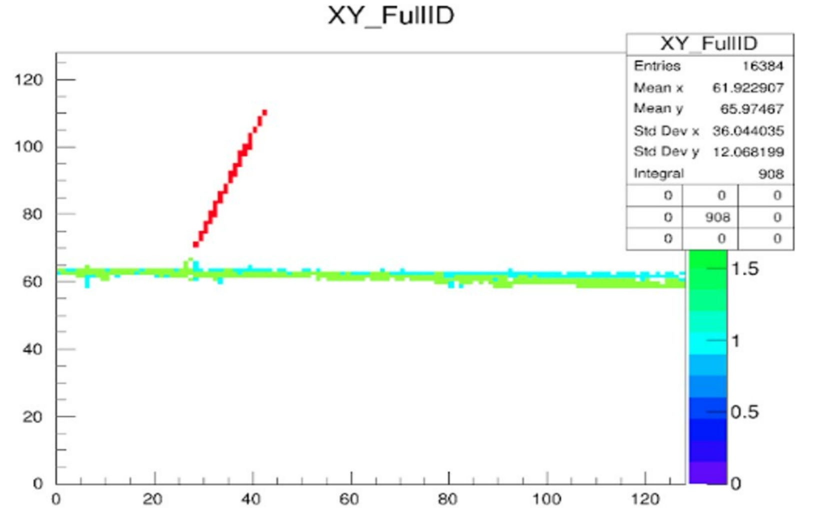

Noisy conditions response:

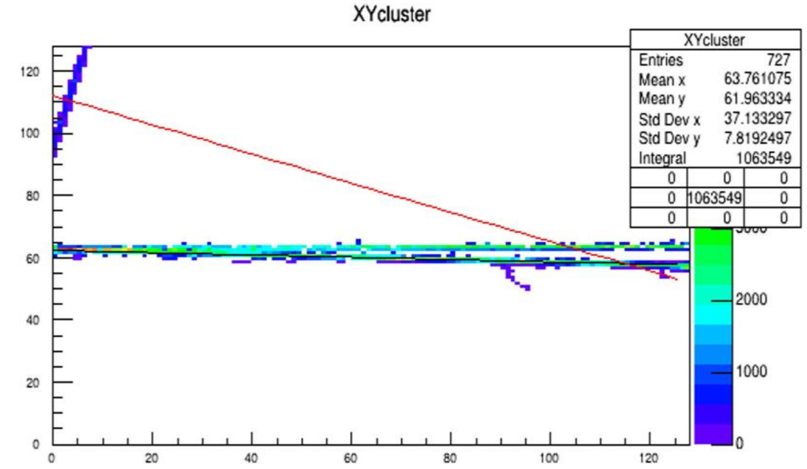

Experimental conditions:

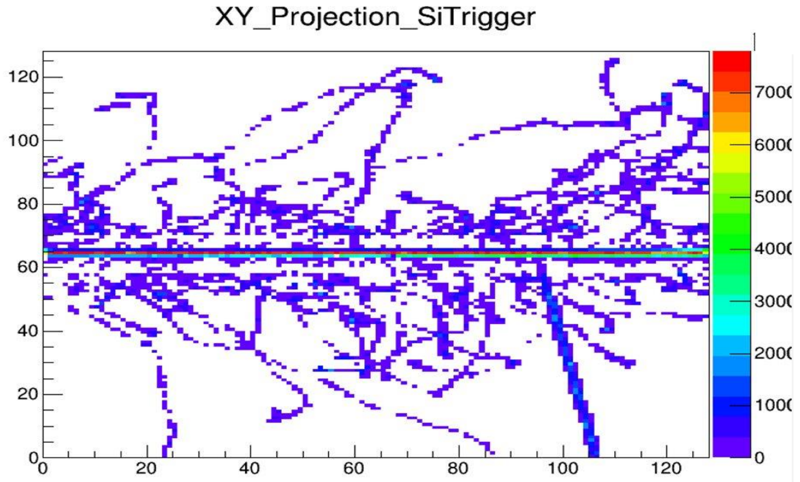

RANSAC Algorithm

RANdom SAmple Consensus

How the algorithm works:

- SAMPLING : sample a small subset of data points, those points will be treated as inliers.
- MODEL PARAMETERS: evaluation of the model parameters:
- SCORE: check on the points number that support the chosen model.

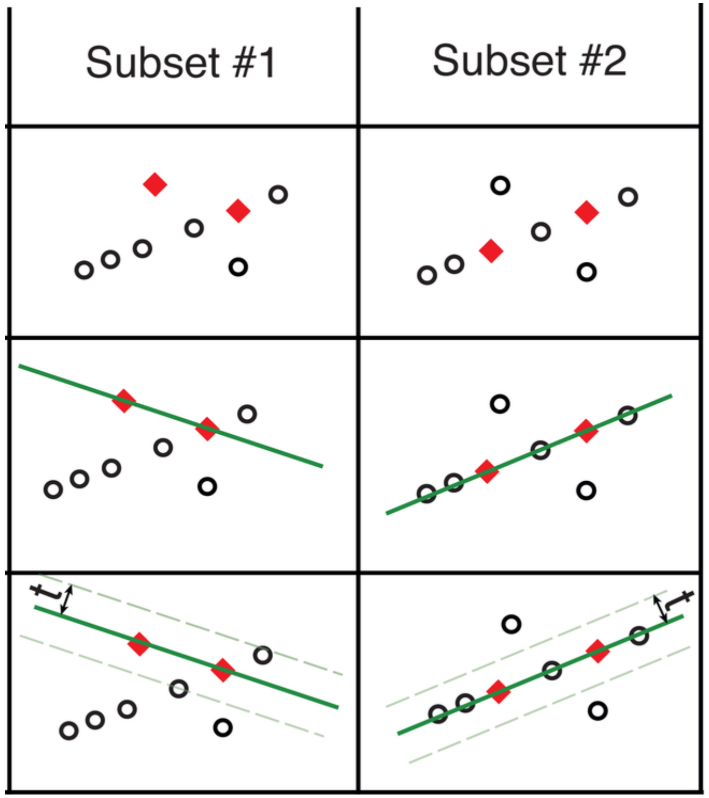

Number of iterations

Fit using RANSAC algorithm

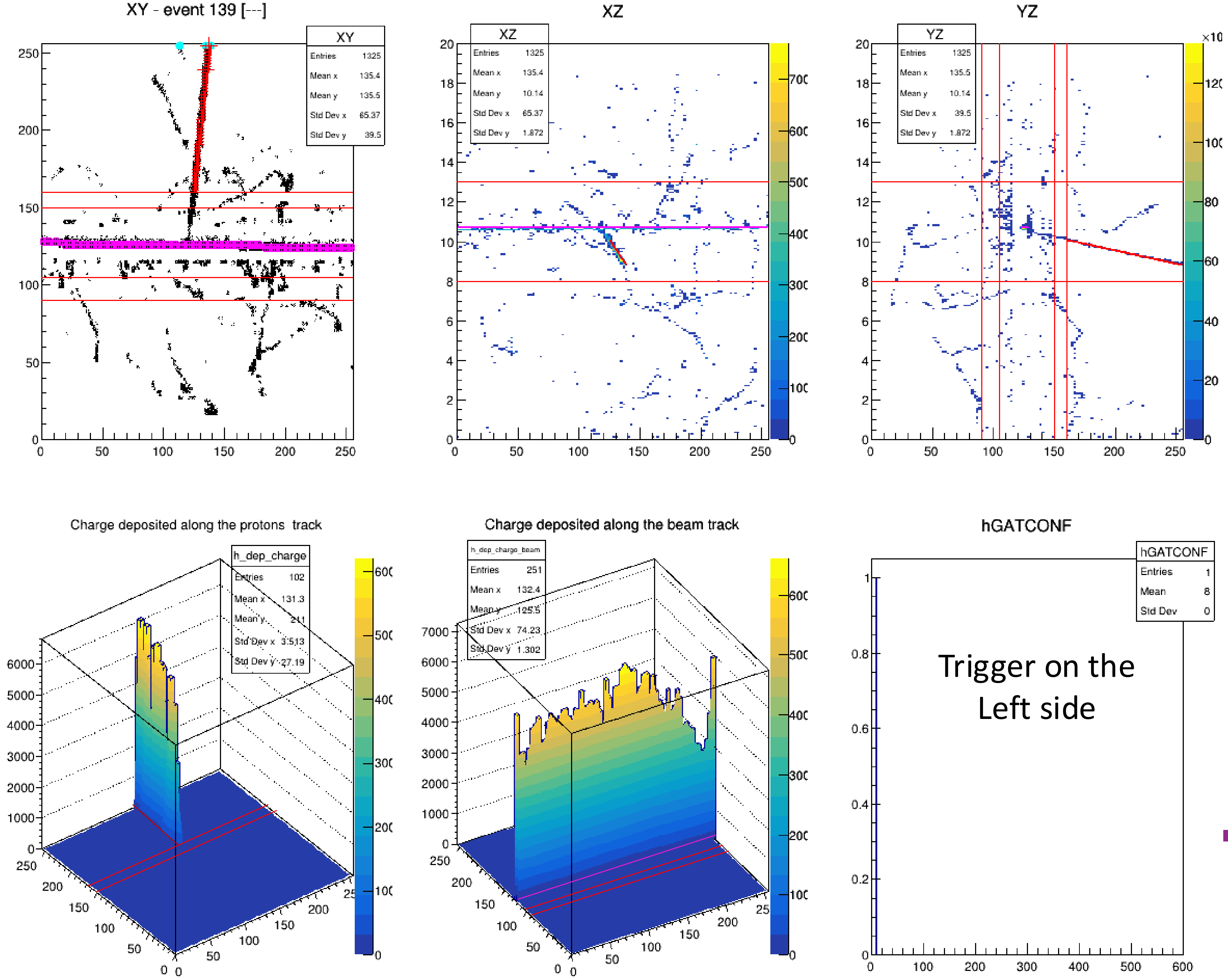

An example of a *scattering event* from ACTAR TPC. Upper part: projections of the signal in the 3 planes. The z-axis corresponds to the time and it's derived using the electron drift velocities.
Bottom part: xy plane projections and the charge deposited along the proton track and along the beam track.

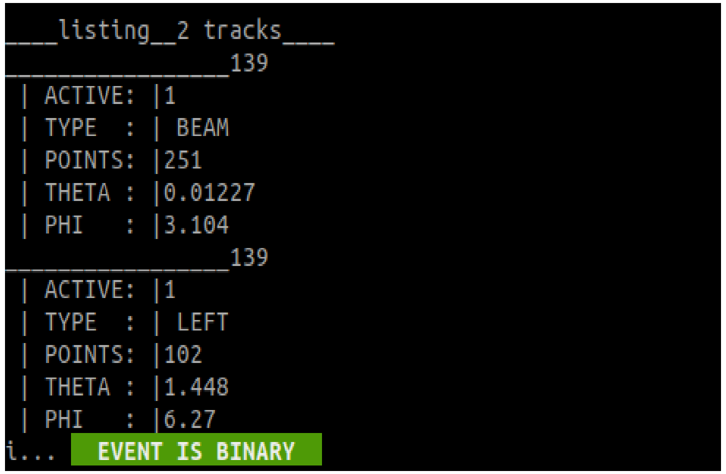

Run 136: 36Si, 1h measurement.
current on CFA 18 nA, VAL = 15 Hz, CFA div = 1:1x10^4

Beam study using RANSAC RECURSIVE algorithm

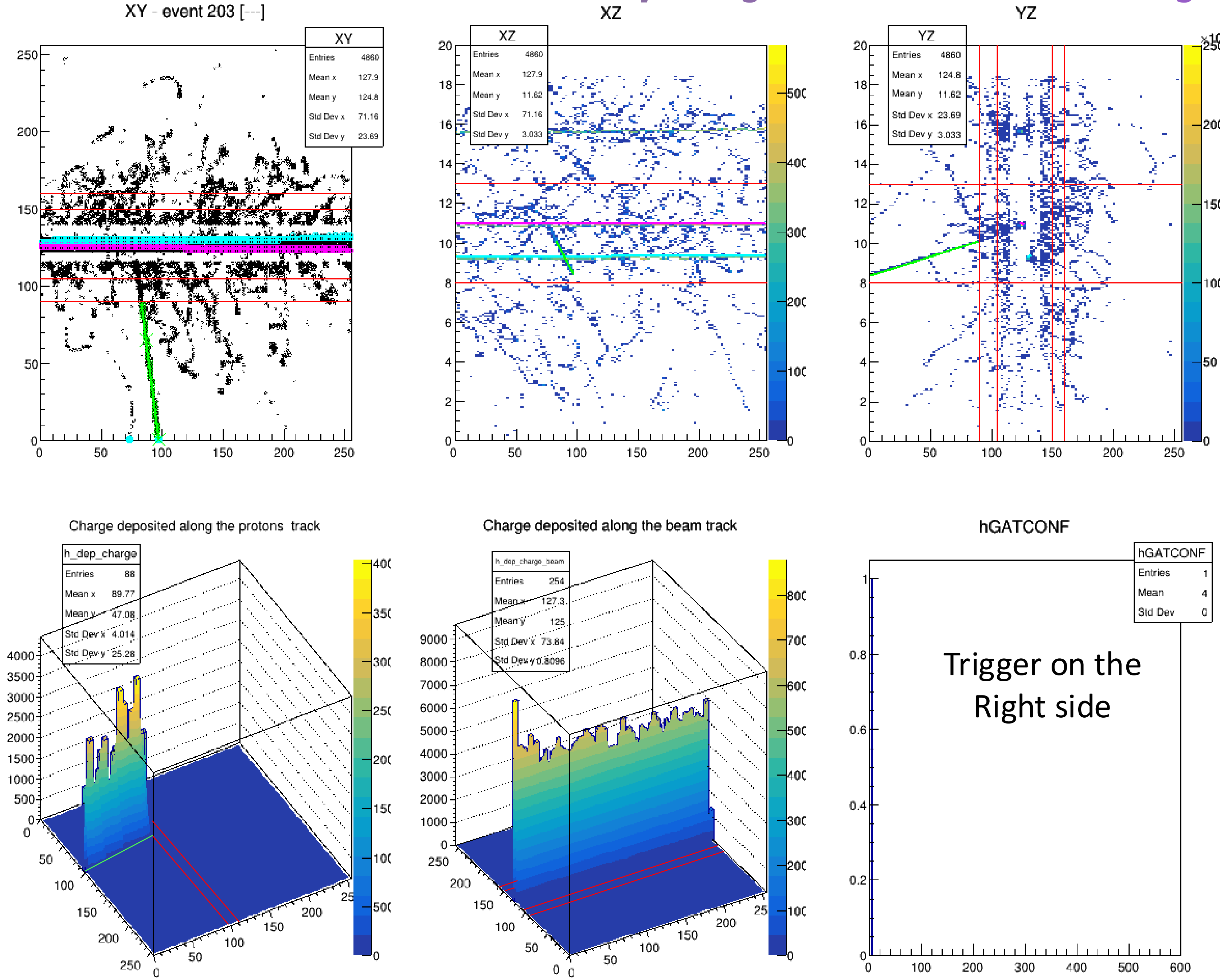

Example of ***pileup event*** observed in ACTAR TPC, two beam tracks are seen and only one proton track. The two beam tracks have different time (z axis). The beam track below corresponds to a previous beam ion. The color scale indicates the charge deposit.

```
0... RETURNED FROM RECURSIVE RANSAC3D with 16 inliers
i... R-TRACKS / TOT-TRACKS: 1 / 3

___listing__3 tracks____
____________________203
| ACTIVE:  |1
| TYPE   : | BEAM
| POINTS:  |254
| THETA  : |0.01193
| PHI    : |3.124
____________________203
| ACTIVE:  |1
| TYPE   : | BEAM
| POINTS:  |232
| THETA  : |0.006498
| PHI    : |0.07066
____________________203
| ACTIVE:  |1
| TYPE   : | RIGHT
| POINTS:  |88
| THETA  : |1.418
| PHI    : |3.162
```

Run 136: 36Si, 1h measurement.
current on CFA 18 nA, VAL = 15 Hz, CFA div = 1:1x10^4

A preliminary example using the 34Si data and applying the cluster algorithm

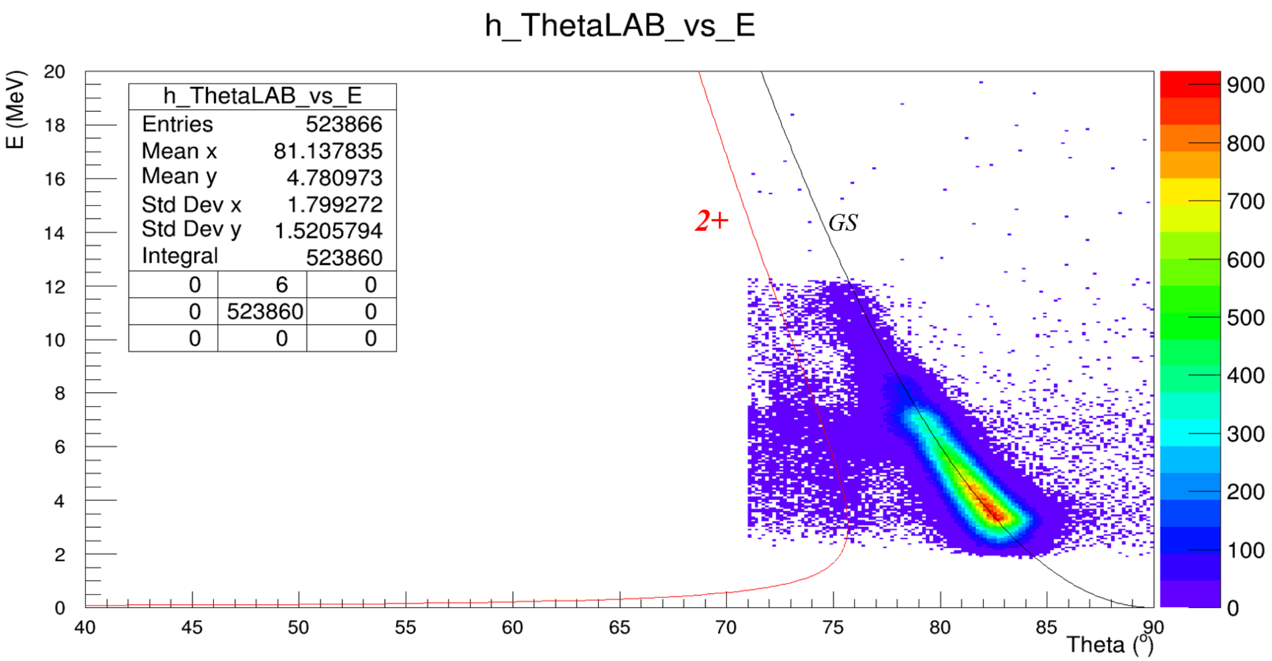

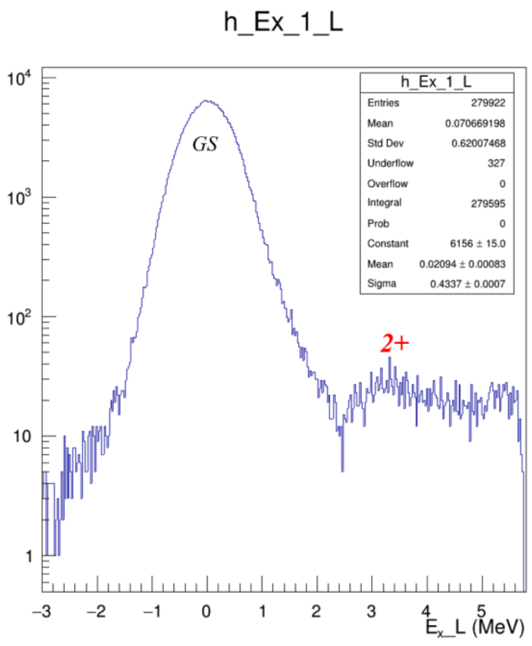

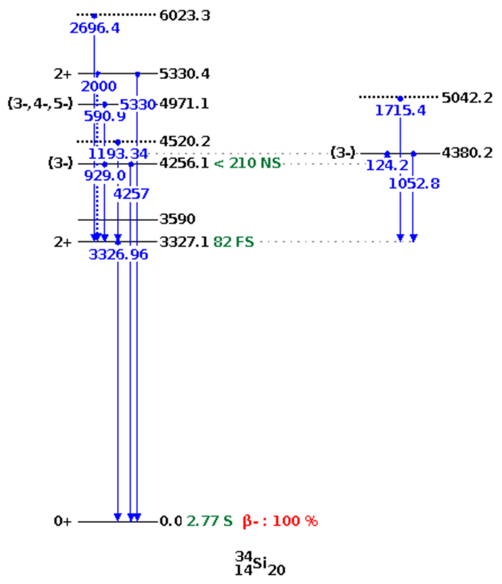

PhD students working on LISE campaign 2022 data

Conclusions

- The **brochette setup** built in GANIL laboratories was presented, with focus on the **ACTAR TPC** detection system;
- The setup allowed us to perform two experiments with the same beam, in fact the goal of the experiment is the evaluation of the *proton and neutron transition matrices* that cannot be extracted using only one probe.
- **Data analysis** structure and status;
- Future code **developments and goals** were discussed.

Tutor: Dr. Jaromir Mrazek, R. Thomas

ACTAR and COULEX collaboration:
F. De Oliveira, J. Pancin, J. Giovinazzo, A. Ortega, B. Fernandez Dominguez, J. Lois Fuentes, S. Grevy, Q. Delignac, K. Shumpei, R. Lica, R.E. Mihai, S. Calinescu

Special thanks to:
all the LISE operational team, all the Cyclotrons teams, all the many others collaborators and the GANIL students that helped during the experimental campaign.

Thank you for your attention!

Nuclear Physics Institute

CHARLES UNIVERSITY
Faculty of mathematics and physics

BARRANDE FELLOWSHIPS

GANIL
GRAND ACCELERATEUR NATIONAL D'IONS LOURDS
LABORATOIRE COMMUN DSM/CEA-IN2P3/CNRS

MINISTERSTVO ŠKOLSTVÍ, MLÁDEŽE A TĚLOVÝCHOVY

Backups

Shell evolution and spin-isospin interaction

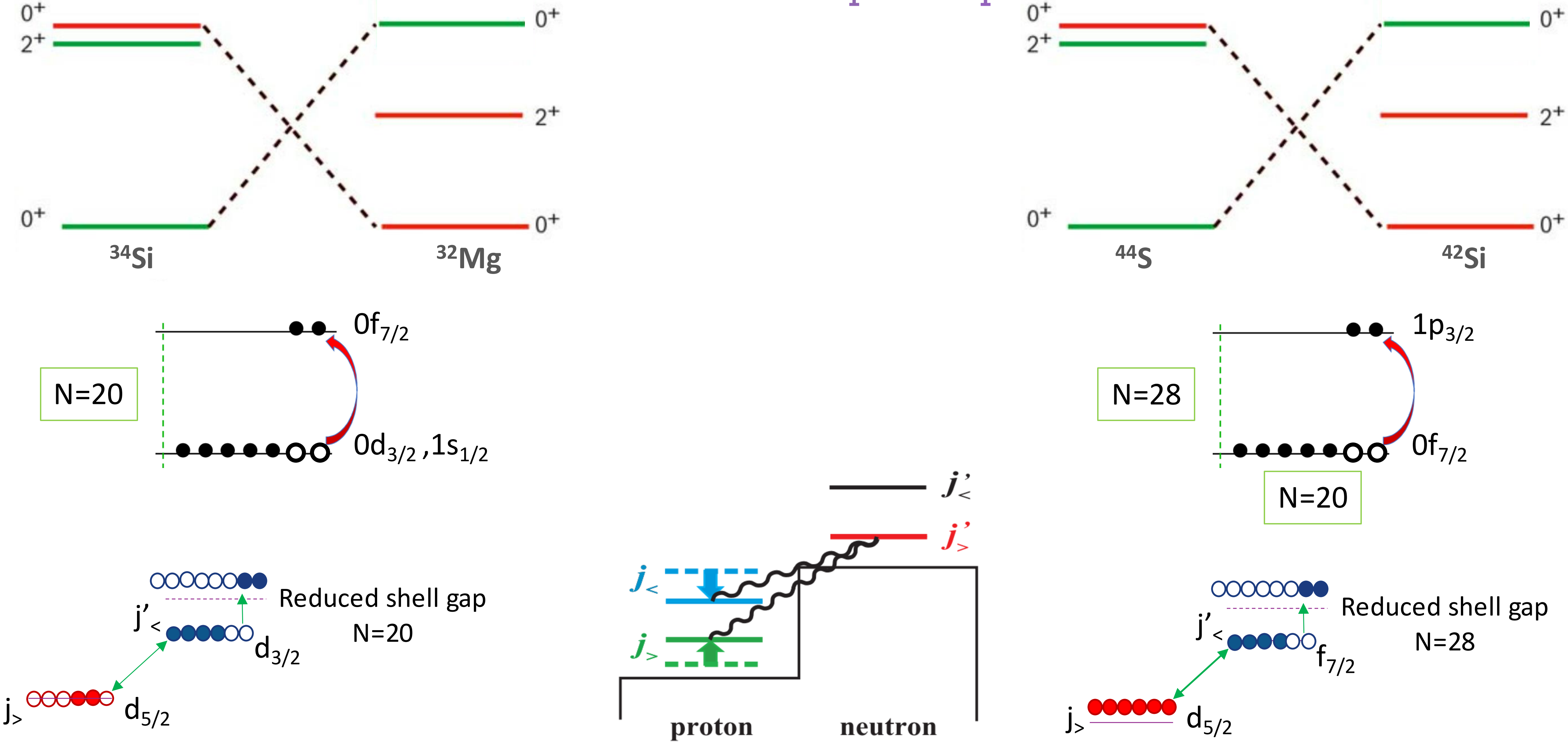

Probing Different Characteristics of Shell Evolution Driven by Central, Spin-Orbit, and Tensor Forces; Yutaka Utsuno; 2022

Derivation of the Mn/Mp ratio in exotic nuclei

- Assumptions:

$$U = U_n + U_p$$

$$R = R_0 + \delta^F$$

- Woods-Saxon shape for the potential:

$$U(R) = \frac{U_0}{1 + e^{r - R_0/a}}$$

$$\Delta U \cong -\frac{\delta^F U_0}{4a}$$

- Optical potential U and transition potential ΔU

$$U(R) = U(R_0 + \delta^F) = U(R_0) + \Delta U$$

$$\frac{\delta^F U_0}{a} = \frac{\delta_p U_p}{a_p} + \frac{\delta_n U_n}{a_n}$$

$$\frac{U_n}{U_p} = \frac{N b_n}{Z b_p}$$

$$\frac{U_n}{U_p} = \frac{\frac{\delta^F a_p}{\delta_p a} - 1}{\frac{\delta_n a_p}{\delta_p a_n} - \frac{\delta^F a_p}{\delta_p a}}$$

- Transition 2+ amplitude

$$M = \langle J_f, T_f, T_{fz} || O_L^F || J_i, T_i, T_{iz} \rangle$$

$$M = b_n^F M_n + b_p^F M_p$$

$$\frac{M_n}{M_p} = \frac{N \beta_n}{Z \beta_p}$$

→

$$\frac{M_n}{M_p} = \frac{b_p}{b_n}\left[\frac{(\beta_p R)_{pp'}}{(\beta_n R)_{em}}\left(1 + \frac{b_n N}{b_p Z}\right) - 1\right]$$

E.Khan. Derivation of the Mn/Mp ratio in exotic nuclei. Phys.Rev.C , 2022, 105, 014306

ACTAR TPC electronics and signal processing

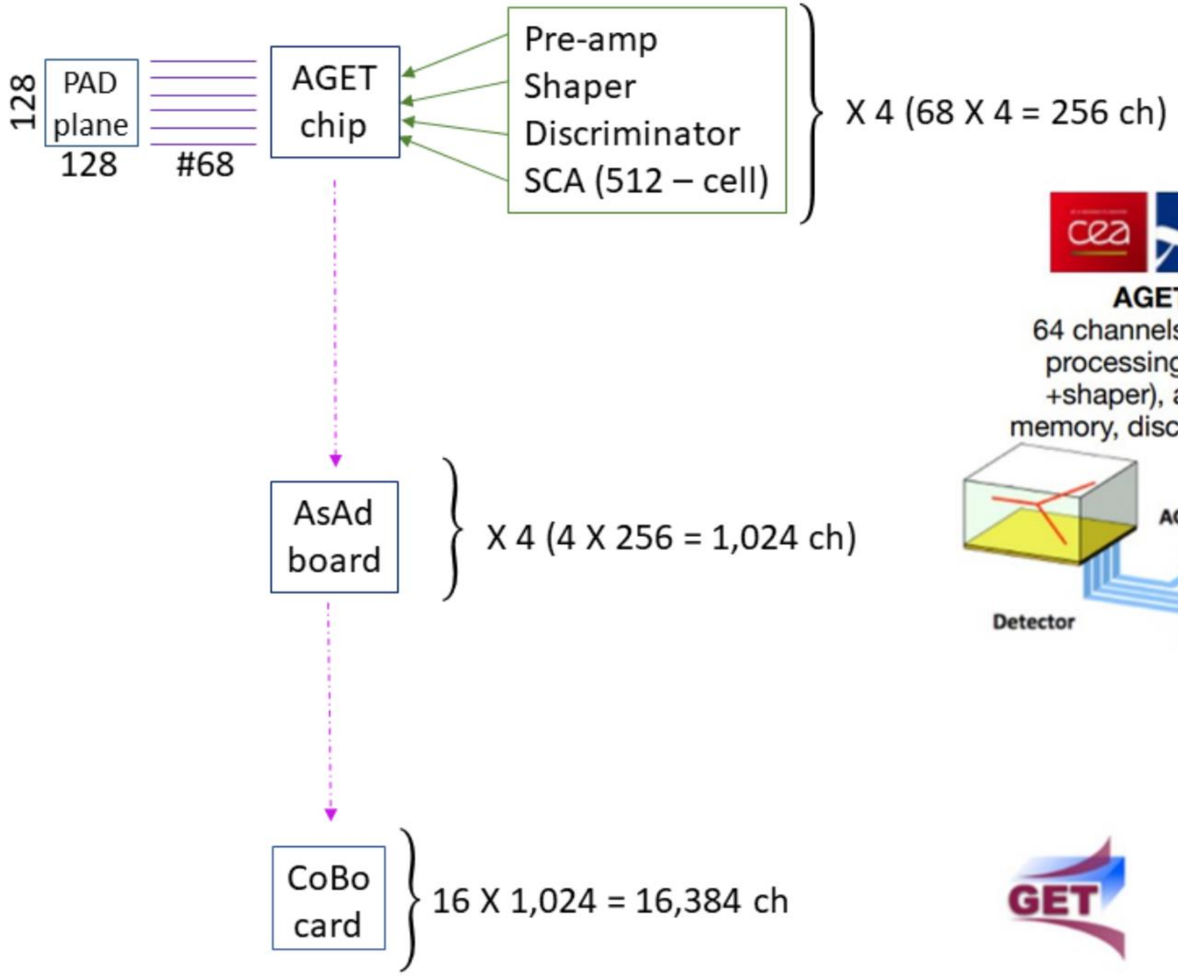

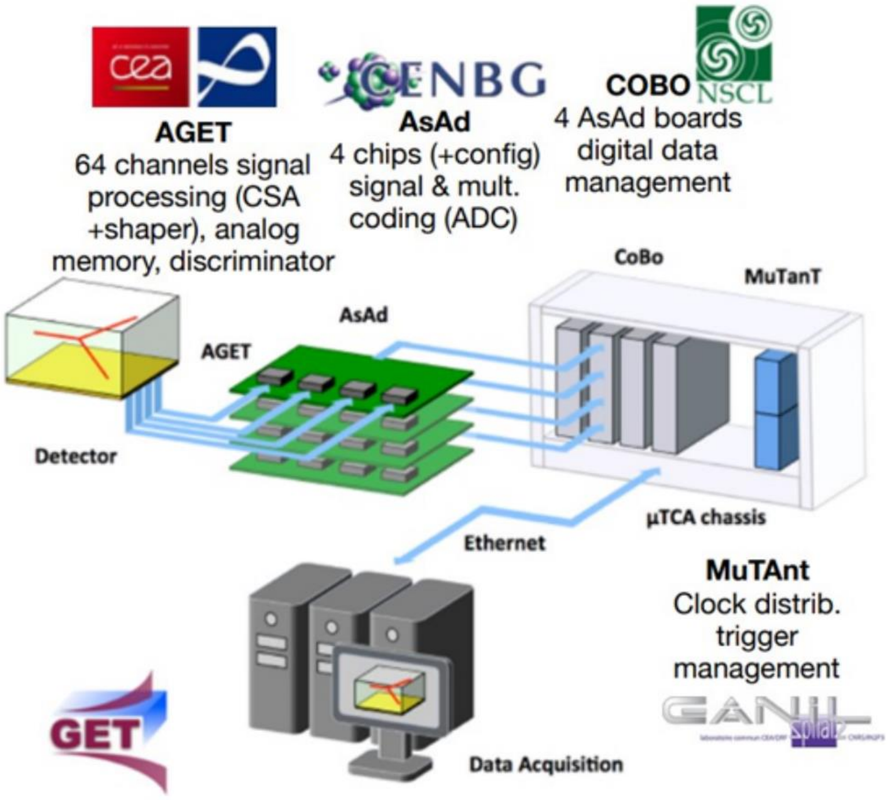

MICROMEGAS calibration for ACTAR TPC; B. Mauss , T. Roger , J. Pancin, S. Damoy, and G. F. Grinyer; 2018

Beam identification

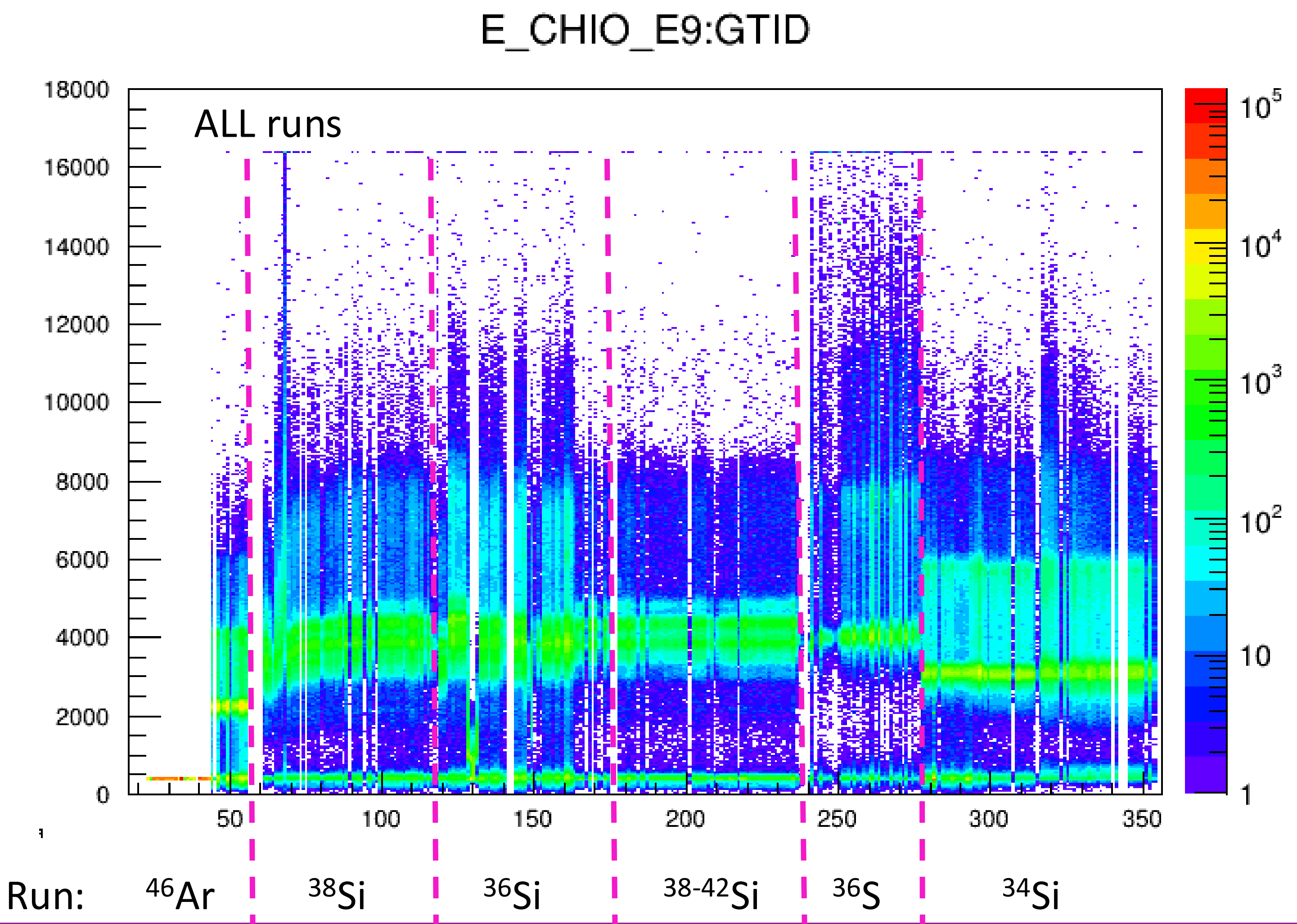

Beam identification

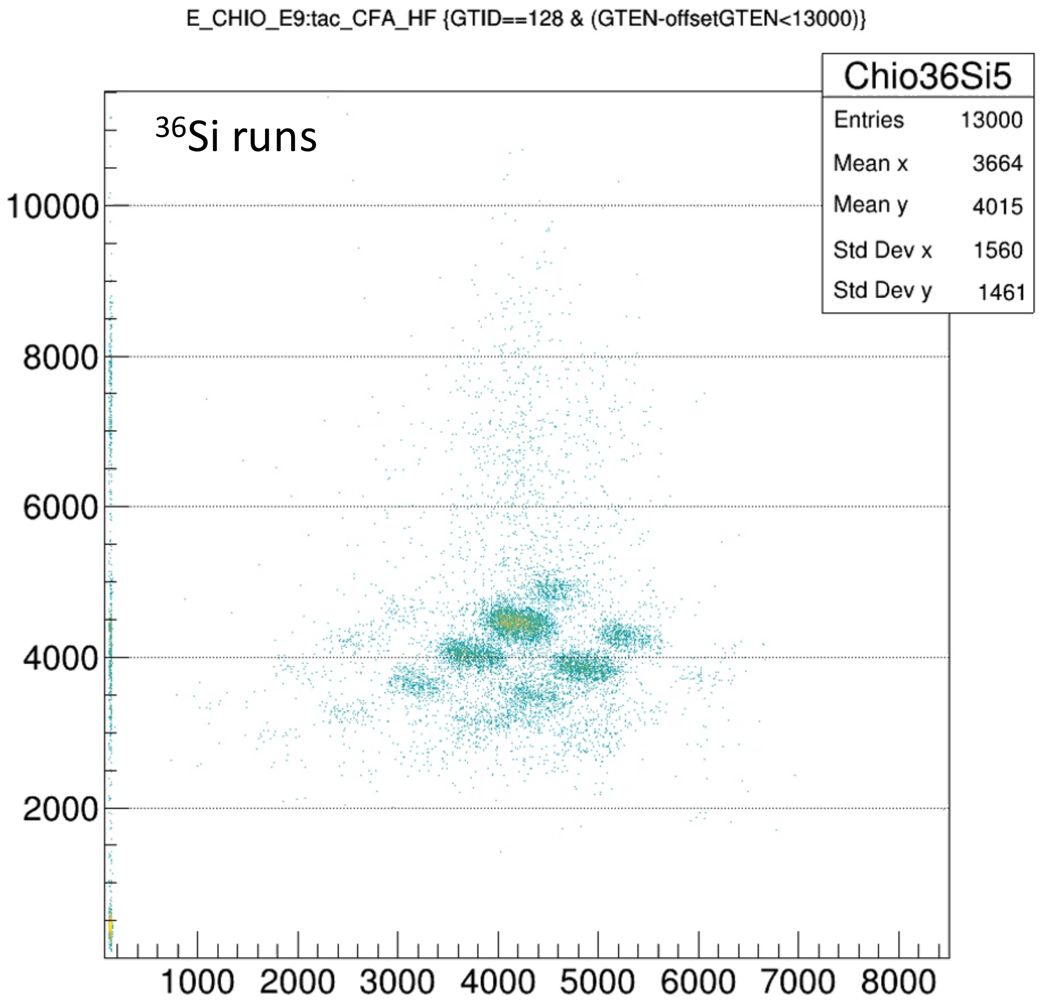

TTree Level 1 : RDataFrame - ROOT's DataFrame

ROOT's RDataFrame offers a modern, high-level interface for analysis of data stored in TTree , CSV and other data formats, in C++ or Python.

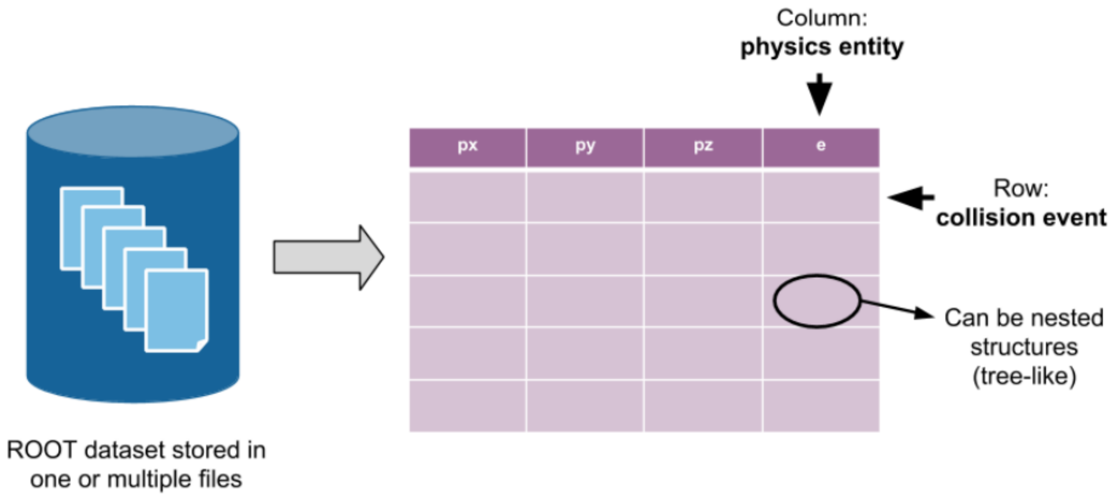

RDataFrame is built with a *modular* and *flexible* workflow in mind, summarised as follows:

1. **Construct a dataframe object** by specifying a dataset. **RDataFrame** supports **TTree** as well as **TChain**, CSV files, SQLite files, RNTuples, and it can be extended to custom data formats.
2. **Transform** the dataframe by:
   - Applying filters. This selects only specific rows of the dataset.
   - Creating custom columns. Custom columns can, for example, contain the results of a computation that must be performed for every row of the dataset.
3. **Produce results**. *Actions* are used to aggregate data into results.

TTree Level 1 :

GLOBAL variables:

- GTID – Global Term for ID (linked to Run number);
- GTEN – Global Term for Entry Number (linked to the Entry number of each run);
- GTTS – Global Term for Time Stamp (linked to the time stamp of each run)

Only one TFile and one TTree for all the runs!

Easy method to overview all the data.

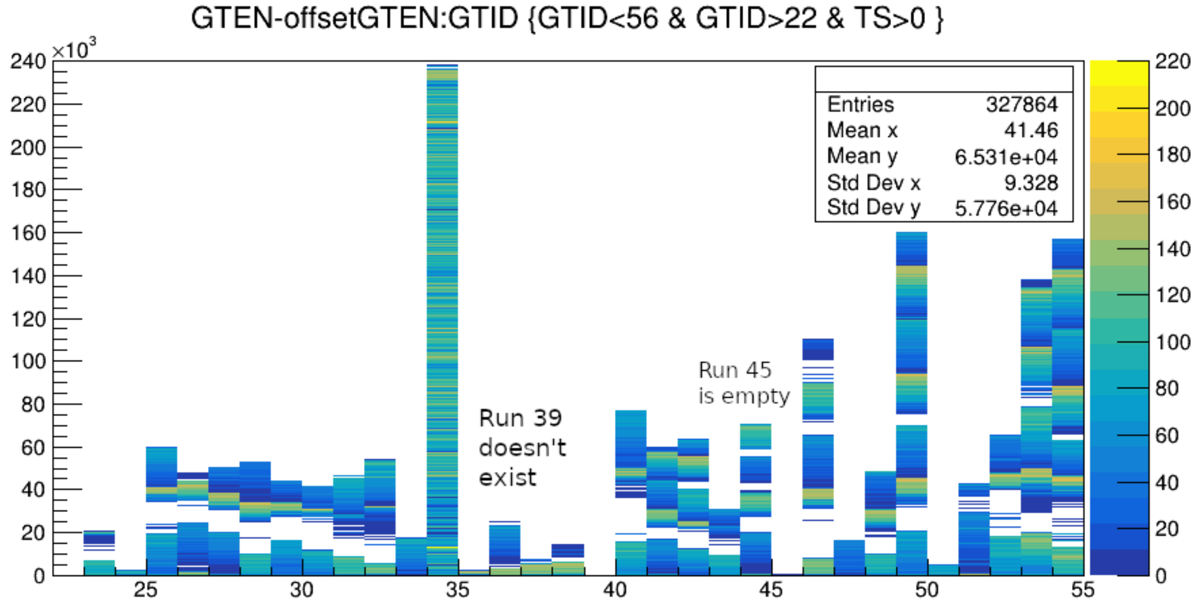

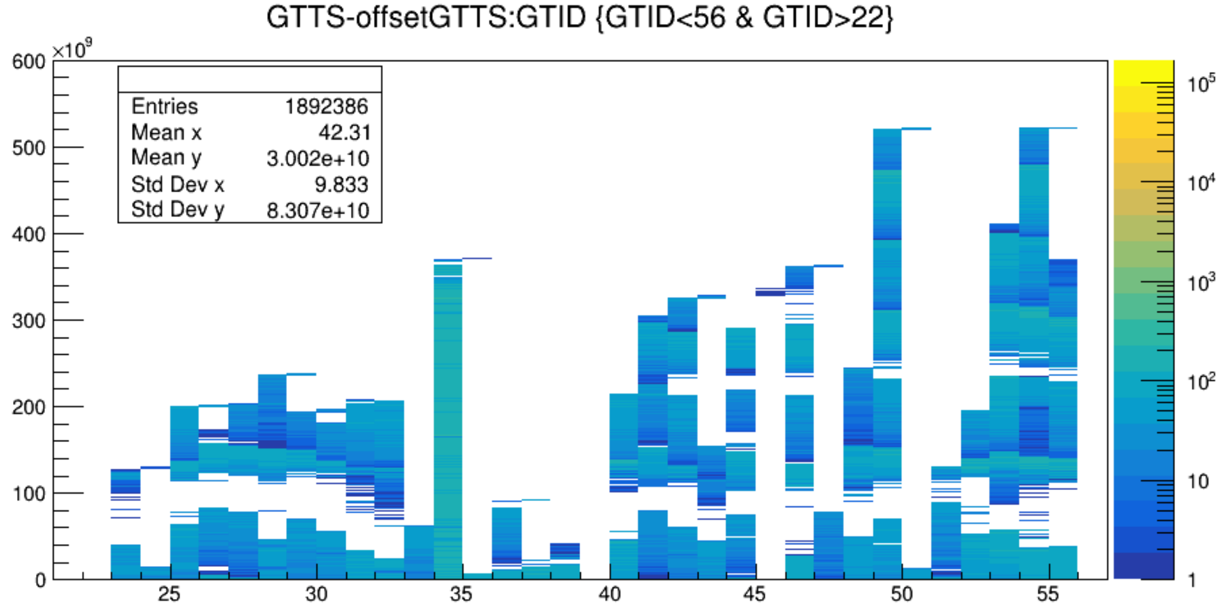

Run 23-55: 46Ar – E[41.9,42.6] MeV/u

TTree Level 1 :

Run 34: 46Ar – E[41.9,42.6] MeV/u

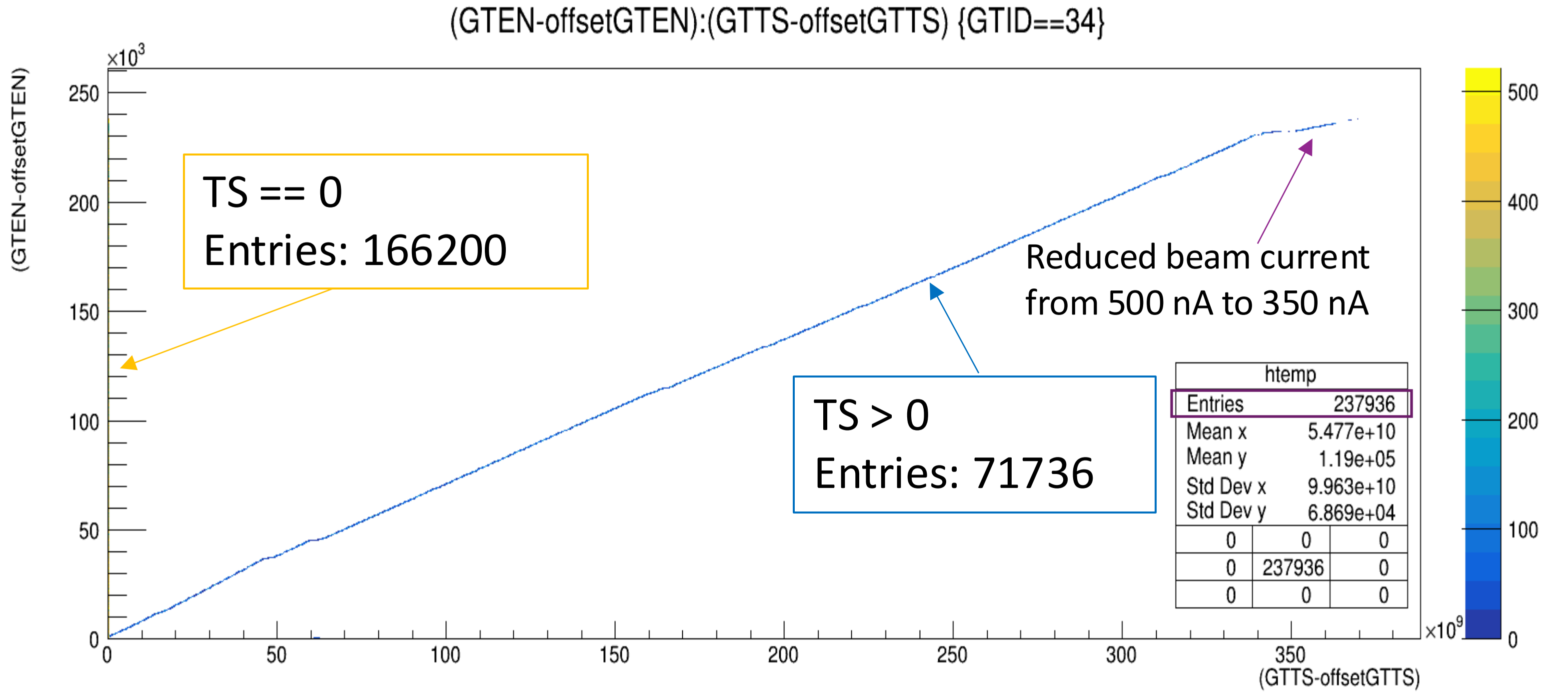

Selected run entries = 237936
All File entries =10365567
Result of cuts on gatconf values:
- gatconf = SiDet: 209804
- gatconf = 4 (Si0R): 62296
- gatconf = 8 (Si0L): 146753
- gatconf = 12 (Si0R + Si0L): 755
- gatconf = 512 (CFA): 28132
- gatconf SiDet + CFA: 237936
- other values of gatconf: 0

- CHIO 'good' events: 133212
- CFA max (N of p.): $340*10^6$

TTree Level 1 :

	46Ar-(run 23-55)	38Si-(run 61-118 + run 165-236)	36Si-(run 119-163)	36S-(run 237-275)	34Si-(run 276-354)
Entries	1892386	2903256	2033198	648832	2866376
trigger Si0L	1130238 - 59.73%	929248 - 32.01 %	821595 - 40.41%	333385 - 51.38 %	1345187 -46.93%
trigger Si0R	507623 - 26.82%	870798 - 29.99 %	723732 - 35.60%	247829 - 38.20 %	1284459 - 44.81%
trigger CFA div	248756 - 13.15%	1094057 - 37.68 %	479536 - 23.59%	64327 - 9.91 %	222071 - 7.75%
trigger Si0L+Si0R	5766 - 0.30%	9125 - 0.31 %	8330 - 0.41%	3290 - 0.51 %	14651 - 0.51%
other values for trigger	3	28	5	1	8
Si det/CFA (trigger)	0.87	0.61	0.75	0.90	0.92
CFA max - medium	$340*10^6$ - $179*10^6$	$72*10^6$ - $38*10^6$	$186*10^6$ - $105*10^6$	$177*10^6$ - $90*10^6$	$219*10^6$ - $120*10^6$
CHIO - good	448424 – 23%	2081916 - 71%	1396587 - 68%	389087 - 60%	6533 – 0.23%

Multitracks study using RANSAC RECURSIVE algorithm

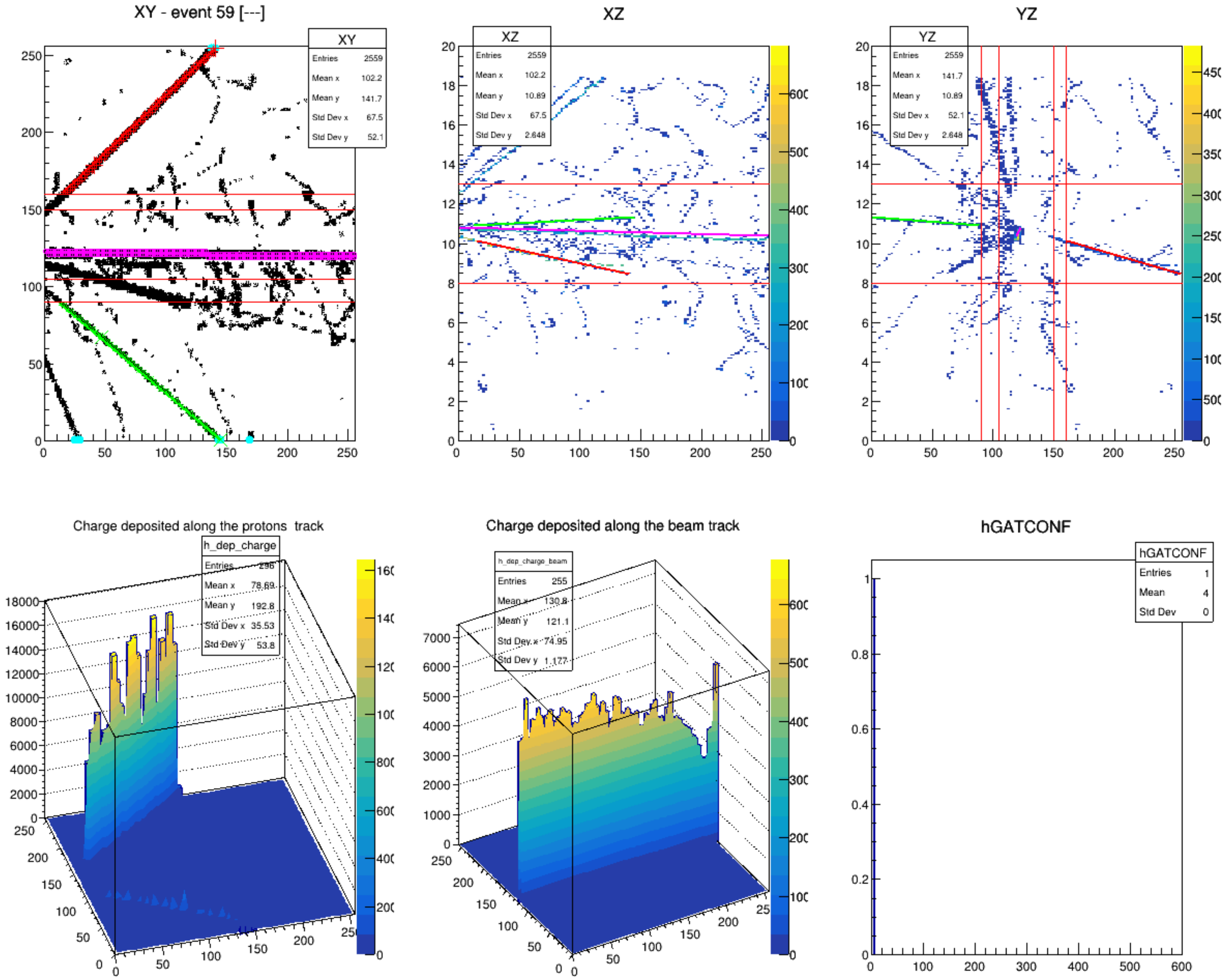


```
D... RETURNED FROM RECURSIVE RANSAC3D with 59 inliers
i... R-TRACKs / TOT-TRACKs: 1 / 3

____listing__3 tracks____
_________________59
 | ACTIVE: |1
 | TYPE   : | BEAM
 | POINTS: |255
 | THETA : |0.01207
 | PHI    : |3.336
_________________59
 | ACTIVE: |1
 | TYPE   : | LEFT
 | POINTS: |158
 | THETA : |0.649
 | PHI    : |6.266
_________________59
 | ACTIVE: |1
 | TYPE   : | RIGHT
 | POINTS: |138
 | THETA : |0.595
 | PHI    : |3.137
```

Run 136: 36Si, 1h measurement.
current on CFA 18 nA, VAL = 15 Hz, CFA div = 1:1x10^4